NEUROSCIENCE

Hippocampal Zkscan4 confers resilience to chronic stress–induced depression-like behaviors

Kai Gao[1,2], Yang Yang[1], Xiaoxuan Sun[1], Jinxin Wang[3], Xiaqin Sun[1], Tianlan Lu[1], Lifang Wang[1], Ming Li[4], Weihua Yue[1,5], Hesheng Liu[2], Dai Zhang[1,2], Jun Li[1]*

Major depression is a prevalent and devastating psychiatric disorder. However, our understanding of the underlying molecular mechanisms is limited. Here, we found reduced expression of zinc finger protein with Krüppel-associated box and SCAN domains 4 (Zkscan4) in the hippocampi of patients with major depressive disorder and stress-susceptible mice. Zkscan4 disruption (*Zkscan4*$^{-/-}$) was sufficient to induce depression-like behaviors following subthreshold social stress. Zkscan4 regulated excitatory synaptic transmission mainly through direct interaction with the *Htr2a* promoter and the recruitment of glucocorticoid receptors for the transcriptional repression of 5-hydroxytryptamine receptor 2a (Htr2a). Reduced excitatory synaptic transmission in the hippocampus and stress susceptibility in *Zkscan4*$^{-/-}$ mice were restored by pharmacological inhibition, genetic knockdown of Htr2a, or overexpression of the amino-terminal SCAN domain of Zkscan4 (Zkscan4$_{1–133}$) in cornus ammonis region 3. Our findings demonstrate an essential role of Zkscan4 in promoting stress resilience, suggesting a potential antidepressant effect of Zkscan4$_{1–133}$.

INTRODUCTION

Major depression (MD), a common mental illness and a leading cause of disability worldwide, is characterized by depressed mood, interest, and pleasure, often accompanied by vegetative symptoms (*1*). Current first-line antidepressants take weeks or months before they achieve full effects. Relapse occurred among one-third of patients within 6 months after antidepressant discontinuation, and another one-third of patients showed poor response to current antidepressants (*2*, *3*). MD is attributable to both genetic and environmental factors, including stressful life events (*4*–*6*). One of the most important risk factors for MD is chronic stress, and maladaptive transcriptional regulation in response to chronic stress is involved in the etiology of MD (*7*–*9*). However, only a few individuals show rapid progression to MD, while most people exhibit resilience to chronic stress. Further understanding of transcriptional regulation implicated in stress resilience might provide more insights into the relevant mechanism and identification of therapeutic targets for MD.

5-hydroxytryptamine receptor 2a (Htr2a), a 5-hydroxytryptamine receptor subtype, is highly expressed in the medial prefrontal cortex (mPFC) (*10*) and moderately expressed in the hippocampus, especially in cornus ammonis region 3 (CA3) and part of CA1 (*11*, *12*). HTR2A is reportedly overexpressed in the brain and peripheral blood of patients with major depressive disorder (MDD) (*13*, *14*), especially in patients resistant to selective serotonin reuptake inhibitors (*15*). Moreover, HTR2A can be down-regulated by chronic use of classical antidepressants (*16*, *17*). These findings suggest that HTR2A plays a critical role in the pathogenesis of MDD and antidepressant treatment. However, the transcriptional mechanism by which HTR2A levels are regulated is largely unclear.

Several recent genome-wide association studies with large sample sizes reported that the zinc finger protein with Krüppel-associated box (KRAB) and SCAN domains 4 (*ZKSCAN4*), which encodes a C_2H_2-zinc finger protein, is significantly associated with MD (*18*–*21*). This association was further confirmed in a transcriptome-wide association study, which indicated that decreased *ZKSCAN4* expression might confer susceptibility to MD (*21*). However, the involvement of *ZKSCAN4* in the onset of depression and the relevant mechanisms of transcriptional regulation remain unclear.

Here, we demonstrate that Zkscan4 directly binds to the *Htr2a* promoter and recruits glucocorticoid receptors (GRs) to repress Htr2a transcription in the hippocampus. Zkscan4 deletion up-regulates the expression of Htr2a at Schaffer collateral (SC)–CA1 synapses, resulting in a specific reduction in the miniature excitatory postsynaptic current (mEPSC) frequency and increased susceptibility to depression-like behaviors in mice. The overexpression of the amino-terminal SCAN domain of Zkscan4$_{1–133}$ in the CA3 region partly inhibits the transcription of Htr2a, thereby ameliorating excitatory synaptic dysfunction and stress-induced depression-like behaviors. In summary, we identified an important mechanism of transcriptional dysregulation that mediates the synaptic dysfunction and depression-like behaviors caused by Zkscan4 deficiency.

RESULTS

Vulnerability to chronic stress is associated with decreased hippocampal Zkscan4

RNAscope showed that *Zkscan4* mRNA was widely expressed across the mouse brain, especially in the hippocampal CA and dentate gyrus (DG) regions (fig. S1A). To further investigate the relevance of Zkscan4 and stressors in mice, we treated C57BL/6J adult male mice with chronic social defeat stress (CSDS), a well-established animal model of depression (*22*). After exposure to CSDS, C57BL/6J mice were divided into susceptible and resilient subgroups based on the social interaction ratio (Fig. 1, A to C), which was confirmed by sucrose preference, forced swimming, and tail suspension tests (fig. S1, B to E). We found that *Zkscan4* mRNA and protein levels in the hippocampus

[1]Peking University Sixth Hospital, Peking University Institute of Mental Health, NHC Key Laboratory of Mental Health (Peking University), National Clinical Research Center for Mental Disorders (Peking University Sixth Hospital), Key laboratory of Mental Health, Chinese Academy of Medical Sciences, Beijing 100191, China. [2]Changping Laboratory, Beijing 102206, China. [3]Chinese Institute for Brain Research, Beijing 102206, China. [4]Yunnan Key Laboratory of Animal Models and Human Disease Mechanisms, Kunming Institute of Zoology, Chinese Academy of Sciences, Kunming 650201, China. [5]PKU-IDG/McGovern Institute for Brain Research, Peking University, Beijing 100871, China.
*Corresponding author. Email: junli1985@bjmu.edu.cn

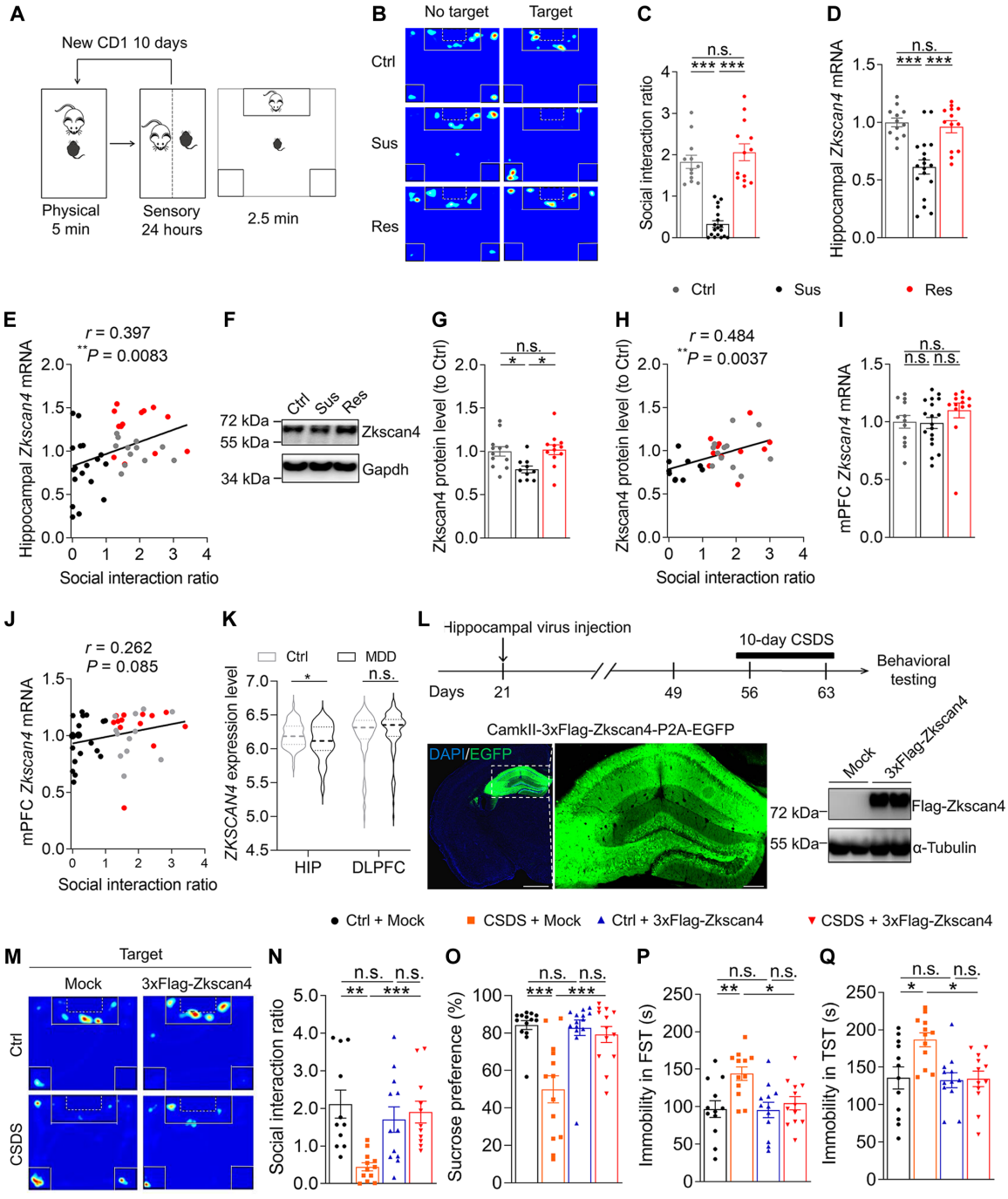

Fig. 1. Reduced hippocampal Zkscan4 expression in stress-susceptible mice and patients with MDD. (**A**) CSDS and social interaction behavioral tests. (**B**) Representative heatmaps of the time spent in the social interaction test. (**C**) Decreased individual social interaction ratio in susceptible (Sus) mice, but not resilient (Res) mice. n.s., not significant. (**D** and **E**) *Zkscan4* mRNA levels were lower in the hippocampi of stress-susceptible mice than in that of control (Ctrl) mice and were correlated with social avoidance. *r*, correlation coefficient. (**F** to **H**) Zkscan4 protein levels were lower in the hippocampi of stress-susceptible mice and correlated with social avoidance. Gapdh, glyceraldehyde-3-phosphate dehydrogenase. (**I** and **J**) Zkscan4 mRNA levels were normal in the mPFC of stress-susceptible mice and were not correlated with social avoidance. (**K**) *ZKSCAN4* mRNA levels were lower in the hippocampus (HIP), but not in the DLPFC, of patients with MDD. HIP ctrl, $n = 72$; HIP MDD, $n = 60$; DLPFC ctrl, $n = 97$; DLPFC MDD, $n = 111$. (**L**) Timeline of virus injection and behavioral studies and representative image of neurons infected with adeno-associated virus (AAV) construct and Zkscan4 protein expression following virus injection in the hippocampi of stress-naive mice. Scale bars, 1 mm (normal magnification) and 200 μm (high magnification). DAPI, 4′,6-diamidino-2-phenylindole. (**M**) Representative heatmaps showing the amount of time spent in the social interaction test after CSDS. (**N** to **Q**) Zkscan4 overexpression in the hippocampus promoted resilience to CSDS-induced depression-like behaviors in C57BL/6J mice, as assessed by the social interaction test, sucrose preference test, forced swimming test (FST), and tail suspension test (TST). All the data are presented as the means ± SEMs. One-way analysis of variance (ANOVA), two-sided Pearson's correlation, and two-tailed Student's *t* test with Welch's correction. $^{*}P < 0.05$; $^{**}P < 0.01$; $^{***}P < 0.001$.

were lower in the susceptible mice than those in the unstressed controls and resilient mice (Fig. 1, D, F, and G). Further analysis indicated a positive association of hippocampal *Zkscan4* mRNA and protein levels with the social interaction ratio (Fig. 1, E and H). In addition, hippocampal *Zkscan4* mRNA was also associated with sucrose preference index, immobility time in forced swimming, and tail suspension tests (fig. S1, F to H). However, *Zkscan4* mRNA levels in the mPFC of susceptible mice were not different from those in the mPFC of unstressed controls or resilient mice (Fig. 1I), and no correlation between *Zkscan4* mRNA and social avoidance behaviors was noted (Fig. 1J), indicating that CSDS-induced Zkscan4 down-regulation is potentially region specific. Furthermore, 28 days, rather than 6 days, of unpredictable chronic mild stress, a widely used non–social stress–induced depressed mouse model, also induces depression-like behaviors with reduced hippocampal *Zkscan4* mRNA (fig. S1, I and J). Last, we analyzed data on *ZKSCAN4* mRNA expression in the hippocampus and dorsolateral prefrontal cortex (DLPFC) of postmortem patients with MDD, which were deposited at the database of Genotypes and Phenotypes (dbGaP; accession number phs000979.v3.p2). *ZKSCAN4* mRNA expression was lower in the hippocampus but not in the DLPFC of patients with MDD compared with healthy controls (Fig. 1K). These findings suggested a cross-species correlation between reduced hippocampal Zkscan4 expression and depression-like phenotypes. Therefore, we hypothesized that *Zkscan4* expression in the hippocampus, but not the prefrontal cortex, plays a critical role in regulating chronic stress–induced depression-like behaviors.

To explore the effect of hippocampal Zkscan4 overexpression on stress-induced depression-like behaviors, we injected an adeno-associated virus (AAV) expressing Zkscan4–enhanced green fluorescent protein (EGFP) driven by the calcium- and calmodulin-dependent protein kinase II (CamkII) promoter into the hippocampus of C57BL/6J mice, which were then allowed to recover for 4 weeks before CSDS (Fig. 1L). After exposure to CSDS for 10 days, the mice injected with AAV-CamkII-EGFP showed notable depression-like behaviors (Fig. 1, M to Q) compared to the unstressed mice; however, depression-like behaviors were not observed in the mice with hippocampal Zkscan4 overexpression (Fig. 1, M to Q, and fig. S1, K and L), suggesting that hippocampal Zkscan4 expression is critical for resilience to chronic stress–induced depression-like behaviors.

Zkscan4 expression in the hippocampus bidirectionally regulates stress-induced depression-like behaviors

To investigate the potential causal role of hippocampal Zkscan4 down-regulation in CSDS-induced depression-like behaviors, we first established a *Zkscan4* knockout (*Zkscan4*$^{-/-}$) mouse model (Fig. 2, A and B, and fig. S2, A to C) that exhibited normal gross morphology of the hippocampus and cortex (fig. S2, D to G). The complexity of dendrites in CA3 pyramidal neurons in unstressed *Zkscan4*$^{-/-}$ mice was comparable with that of their wild-type (WT) littermates; however, the dendritic morphology of CA3 pyramidal neurons in *Zkscan4*$^{-/-}$ mice was reduced after 4 days of subthreshold CSDS (SCSDS) (fig. S2, H and I). Baseline depression-like behaviors were assessed but not observed in *Zkscan4*$^{-/-}$ mice that had not experienced any stress (Fig. 2, D to J). Then, *Zkscan4*$^{-/-}$ mice were subjected to SCSDS, which was not sufficient to induce depression-like behaviors in their WT (*Zkscan4*$^{+/+}$) littermates (Fig. 2C). We found that stressed *Zkscan4*$^{-/-}$ mice spent less time in social interaction with unfamiliar CD1 mice (Fig. 2, D and E) and traveled a normal distance (Fig. 2F). They also showed anhedonia, as assessed by the sucrose preference test (Fig. 2G), but their total fluid consumption was not affected (Fig. 2H). Moreover, *Zkscan4*$^{-/-}$ mice had more immobility time in the forced swimming test (Fig. 2I) and tail suspension test (Fig. 2J). In addition, *Zkscan4*$^{-/-}$ mice exhibited much longer escape latencies and a greater number of escape failures than their WT littermate controls in the learned helplessness paradigm (Fig. 2, K and L) (*23*). These results suggested that *Zkscan4*$^{-/-}$ mice were vulnerable to stress-induced depression-like behaviors.

Locomotor activity was normal (fig. S3A), and anxiety-like behaviors (fig. S3, B to D) were also not observed in *Zkscan4*$^{-/-}$ mice, regardless of whether they experienced stress. The general learning ability and memory of the *Zkscan4*$^{-/-}$ mice were also normal in the novel object recognition (fig. S3E), Y maze (fig. S3, F and G), fear conditioning (fig. S3H), and Barnes maze (fig. S3, I and J) tests.

To further explore whether reexpression of Zkscan4 in the hippocampus can rescue susceptibility to stress, we injected AAV containing CamkII-driven Zkscan4-EGFP into the hippocampi of *Zkscan4*$^{-/-}$ mice aged 3 weeks, and controls were injected with AAV-CamkII-EGFP (Fig. 2M). As expected, compared with WT mice, *Zkscan4*$^{-/-}$ mice treated with AAV-CamkII-EGFP displayed notable social avoidance, as measured by the social interaction ratio, whereas *Zkscan4*$^{-/-}$ mice injected with AAV-CamkII-Zkscan4-EGFP did not show social avoidance after SCSDS (Fig. 2, N and O, and fig. S4A). In addition, SCSDS-induced anhedonia (Fig. 2P and fig. S4B), despair in forced swimming (Fig. 2Q) and tail suspension (Fig. 2R), and foot shock–induced learned helplessness behavior (Fig. 2, S and T) were also improved by Zkscan4 reexpression in the hippocampi of *Zkscan4*$^{-/-}$ mice. These results suggested that hippocampal Zkscan4 expression bidirectionally regulates stress-induced depression-like behaviors.

Loss of Zkscan4 leads to Htr2a up-regulation and synaptic dysfunction

To identify the downstream targets of Zkscan4 in mediating resistance to depression-like behaviors, we isolated the hippocampi of adult *Zkscan4*$^{-/-}$ mice and their littermates after exposure to SCSDS and performed RNA sequencing (RNA-seq). A cutoff of $P < 0.05$ and $|\text{fold change}| \geq 1.5$ was used to identify differentially expressed genes (Fig. 3A). As Zkscan4 mainly acts as a transcriptional repressor, we focused on gene up-regulation in *Zkscan4*$^{-/-}$ mice. *Zkscan4* knockout caused the up-regulation of 209 genes (data S1) that were enriched in signaling pathways according to the Gene Ontology (GO) database with a cutoff of $q \leq 0.05$, especially genes related to synaptic organization, assembly, and transmission (Fig. 3B). To explore whether *Zkscan4* disruption alters synaptic function, we conducted the whole-cell recordings in CA1 pyramidal neurons from nonstressed mice. By recording mEPSCs, we found that the frequency, rather than the amplitude, of mEPSCs was lower in *Zkscan4*$^{-/-}$ mice than in their WT littermates (Fig. 3, C to E). However, neither the frequency nor the amplitude of miniature inhibitory postsynaptic currents (mIPSCs) differed between the two genotypes (fig. S4, C to E). These results indicated that excitatory synaptic transmission in the hippocampus was affected by Zkscan4 disruption.

Among the up-regulated genes in *Zkscan4*$^{-/-}$ mice, Htr2a up-regulation (approximately 1.5-fold) was validated at the individual gene level by quantitative real-time polymerase chain reaction (PCR) and Western blotting in unstressed *Zkscan4*$^{-/-}$ mice (Fig. 3, F to H). In addition, Htr2a mRNA level in the hippocampi of *Zkscan4*$^{-/-}$ mice was twofold greater than that in the hippocampi of WT controls

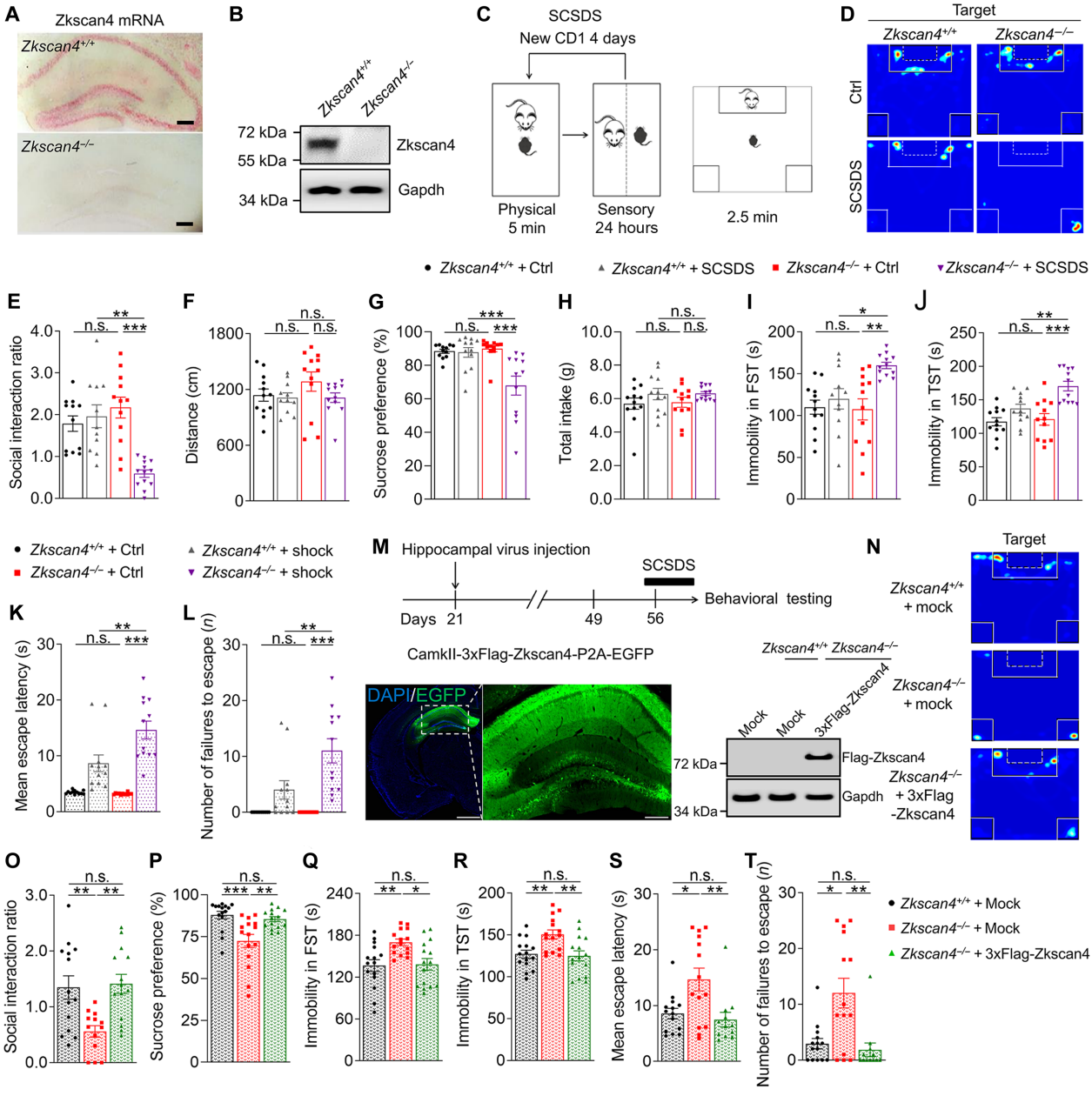

Fig. 2. Zkscan4 disruption is sufficient to induce depression-like behaviors, and Zkscan4 reexpression in the hippocampus restores depression-like behaviors. (**A** and **B**) *Zkscan4* mRNA and Zkscan4 protein cannot be detected in the hippocampi of stress-naive *Zkscan4*$^{-/-}$ mice compared to their littermates. Scale bar, 200 μm. (**C**) Four days of treatment with SCSDS and social interaction behavioral tests. (**D**) Representative heatmaps showing the amount of time spent in the social interaction test after SCSDS. (**E** to **J**) *Zkscan4* knockout in mice treated with SCSDS induced depression-like behaviors, as assessed using the social interaction test, sucrose preference test, forced swimming test, and tail suspension test. The effect was compared to that in unstressed mice and stressed *Zkscan4*$^{+/+}$ mice. (**K** and **L**) *Zkscan4* knockout in mice after unpredictable and inescapable foot shocks induced learned helplessness behaviors, as assessed by mean escape latencies and the number of failures to escape. (**M**) Timelines of the virus injection and behavioral studies, representative image of neurons infected with AAV construct, and Zkscan4 protein following virus injection in the hippocampus of stress-naive mice. Scale bars, 1 mm (normal magnification) and 200 μm (high magnification). (**N**) Representative heatmaps showing the amount of time spent in the social interaction test after SCSDS. (**O** to **R**) Zkscan4 reexpression in the hippocampus reversed SCSDS-induced depression-like behaviors in *Zkscan4*$^{-/-}$ mice, as assessed by the social interaction test, sucrose preference test, forced swimming test, and tail suspension test. (**S** and **T**) Zkscan4 reexpression in the hippocampus reversed the learned helplessness behaviors in *Zkscan4*$^{-/-}$ mice induced by unpredictable and inescapable foot shocks, as assessed using the mean escape latency and the number of failures to escape. All data are presented as the means ± SEMs. One-way ANOVA. **P* < 0.05; ***P* < 0.01; ****P* < 0.001.

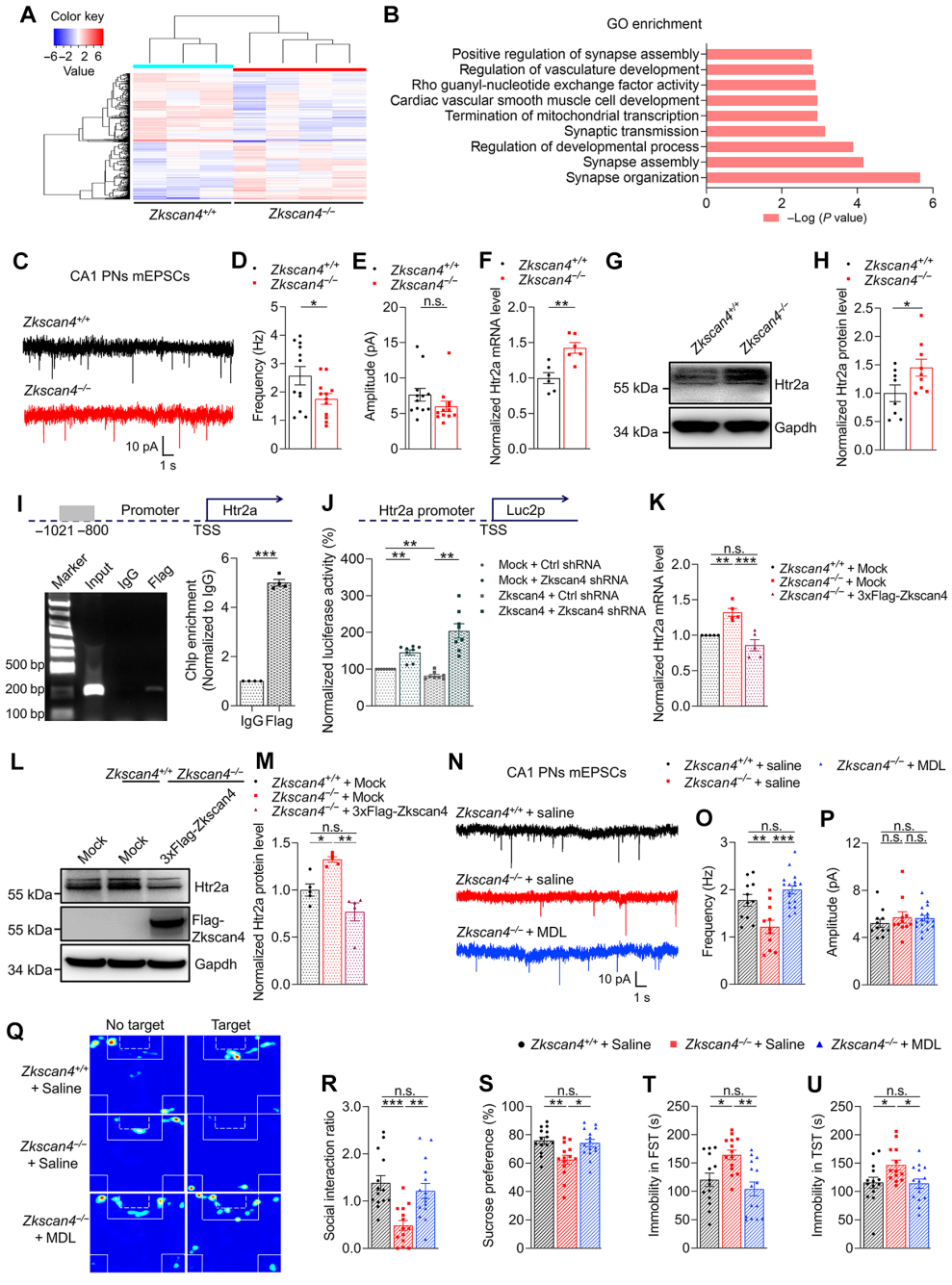

Fig. 3. Loss of Zkscan4 expression leads to Htr2a up-regulation and excitatory transmission dysfunction, and pharmacological blockade of Htr2a rescues synaptic dysfunction and depression-like behaviors. (**A**) Clustering of all differentially expressed genes (DEGs) in the hippocampus of *Zkscan4*$^{-/-}$ mice and their littermates. The red and blue colors indicate up- and down-regulation, respectively. (**B**) GO enrichment of DEGs. The enriched pathways were mainly related to synapse organization and assembly and synaptic transmission. (**C**) Representative traces of mEPSCs recorded in hippocampal slices from *Zkscan4*$^{-/-}$ and *Zkscan4*$^{+/+}$ mice. PNs, pyramidal neurons. (**D** and **E**) Loss of *Zkscan4* led to decreased mEPSC frequency, but not mEPSC amplitude. (**F** to **H**) Htr2a up-regulation in the hippocampi of *Zkscan4*$^{-/-}$ mice as assessed using reverse transcription quantitative polymerase chain reaction (RT-qPCR) and Western blotting. (**I**) Chromatin immunoprecipitation with an anti-Flag antibody showed that Zkscan4-Flag directly binds to the Htr2a promoter. TSS, transcription start site; IgG, immunoglobulin G; bp, base pair. (**J**) Dual-luciferase experiments demonstrated that Zkscan4 repressed the transcription of Htr2a. Luc2p, destabilized and optimized firefly luciferase with the -Pro-Glu-Ser-Thr sequence. (**K** to **M**) In vivo confirmation of the transcriptional repression of hippocampal Htr2a by Zkscan4, as measured using RT-qPCR and Western blotting. (**N**) Representative traces of mEPSCs recorded in hippocampal slices from different groups of mice. MDL, MDL100907. (**O** and **P**) MDL100907 improved the frequency of mEPSCs in CA1 pyramidal neurons of *Zkscan4*$^{-/-}$ mice but did not affect the amplitude. (**Q**) Representative heatmaps showing the amount of time spent in the social interaction test after SCSDS. (**R** to **U**) Pharmacological inhibition of Htr2a reversed SCSDS-induced depression-like behaviors in *Zkscan4*$^{-/-}$ mice, as assessed using a social interaction test, sucrose preference test, forced swimming test, and tail suspension test. All the data are presented as the means ± SEMs. Two-tailed Student's *t* test and one-way ANOVA. **P* < 0.05; ***P* < 0.01; ****P* < 0.001.

after SCSDS (fig. S4F), suggesting that social stress might further increase the transcription of Htr2a in *Zkscan4*$^{-/-}$ mice. To determine whether the Htr2a gene is a direct target of Zkscan4, we performed chromatin immunoprecipitation (ChIP) using a stably transfected Zkscan4-Flag cell line and found that the *Htr2a* promoter was immunoprecipitated by an anti-Flag antibody (Fig. 3I), which was also detected in vivo (fig. S4G). Moreover, a dual luciferase assay using the L929 cell line also showed that Zkscan4 overexpression inhibited luciferase activity controlled by the *Htr2a* promoter and that Zkscan4 knockdown increased luciferase activity (Fig. 3J), indicating that Htr2a might represent a direct target of Zkscan4 and that its expression could be inhibited by Zkscan4. Reexpression of Zkscan4 in the hippocampi of *Zkscan4*$^{-/-}$ mice also restored Htr2a mRNA and protein levels (Fig. 3, K to M). These results indicated that Htr2a transcription is directly regulated by Zkscan4. Moreover, to explore whether there are regional differences between CA1 and CA3 pyramidal neurons in their response to chronic stress, we isolated the CA3 and CA1 regions from the hippocampi of Thy1-GFP mice (with or without CSDS; fig. S4H) and found that both *Zkscan4* and *Htr2a* were substantially altered in both CA3 and CA1 pyramidal neurons from mice exposed to CSDS when compared with controls (fig. S4, I to N). *Zkscan4* mRNA was inversely correlated with *Htr2a* mRNA in both CA3 and CA1 pyramidal neurons (fig. S4, K and N), suggesting that Zkscan4 transcriptionally represses *Htr2a* in the pyramidal neurons across the hippocampus.

Htr2a antagonism restores synaptic and behavioral abnormalities in *Zkscan4*$^{-/-}$ mice

As Htr2a was identified as a downstream transcriptional target of Zkscan4, we examined whether Htr2a was involved in the Zkscan4-mediated regulation of synaptic dysfunction and depression-like behaviors. As expected, the decrease in the frequency of mEPSCs in CA1 pyramidal neurons was reversed by bath application of the Htr2a antagonist MDL100907 (1 μM) (Fig. 3, N to P). Intraperitoneal injection (1.0 mg/kg) of MDL100907 30 min before SCSDS reduced social avoidance, anhedonia, and despair behaviors in *Zkscan4*$^{-/-}$ mice (Fig. 3, Q to U, and fig. S4, O and P). However, MDL100907 treatment for 10 days before behavioral tests had no effect on CSDS-induced depression-like behaviors in C57BL/6J mice (fig. S4, Q to U). In addition, MDL100907 treatment cannot reverse the decreased frequency of mEPSC in CA1 pyramidal neurons from susceptible C57BL/6J mice exposed to CSDS (fig. S4, V to X). These results suggested that Htr2a up-regulation is involved in glutamatergic synaptic dysfunction and subthreshold stress–induced depression-like behaviors in *Zkscan4*$^{-/-}$ mice.

Htr2a knockdown restores synaptic and behavioral abnormalities in *Zkscan4*$^{-/-}$ mice

RNAscope analysis revealed that Htr2a was mainly expressed in CA3 and CA1 pyramidal cells but not in DG granule cells in the hippocampus (fig. S5A). To further investigate the exact region of Htr2a in stress-induced depression-like behaviors and CA3-CA1 synaptic dysfunction in *Zkscan4*$^{-/-}$ mice, we injected AAV-mediated Htr2a short hairpin RNA (shRNA) into the CA3 or CA1 region for Htr2a knockdown (Fig. 4, A and B). The CA3 knockdown of Htr2a reduced SCSDS-induced social avoidance, anhedonia, and despair behaviors in *Zkscan4*$^{-/-}$ mice (Fig. 4, C to G) without affecting locomotion or total fluid intake (fig. S5, B and C). The decrease in the frequency of mEPSCs in CA1 pyramidal neurons was also reversed by the knockdown of Htr2a in CA3 (Fig. 4, H to J). In addition, to enhance the CA3-CA1 synaptic drive, we delivered the AAV-CamkII-Gq-coupled human M3 muscarinic designer receptor exclusively activated by designer drug (hM3Dq) -EGFP/AAV-CamkII-EGFP virus into the CA3 region (fig. S5D). Clozapine N-oxide intraperitoneal injection (1.0 mg/kg) 30 min before SCSDS prevented stress-induced depression-like behaviors in *Zkscan4*$^{-/-}$ mice (fig. S5, E to G). However, knockdown of Htr2a in the CA1 region (Fig. 4, K and L) did not ameliorate stress-induced depression-like behaviors (Fig. 4, M to Q, and fig. S5, H and I) or excitatory synaptic dysfunction in *Zkscan4*$^{-/-}$ mice (Fig. 4, R to T). These results indicated that CA3, but not CA1, Htr2a up-regulation plays an important role in stress-induced depression-like behaviors and synaptic dysfunction in *Zkscan4*$^{-/-}$ mice.

Zkscan4$_{1-133}$ ameliorates synaptic dysfunction and depression-like behaviors in *Zkscan4*$^{-/-}$ mice

Zkscan4 is a member of the KRAB zinc fingers, which function as transcriptional repressors. It has been reported that human ZKSCAN4 interacts with GRs (*24*). First, a coimmunoprecipitation assay demonstrated that mouse Zkscan4 interacts with mouse glucocorticoid receptor (Gr) (Fig. 5A). After the cells were treated with dexamethasone, the interaction between Zkscan4 and Gr increased (fig. S6, A to D). Using a dual luciferase reporter assay on the L929 cell line transiently transfected with the mouse mammary tumor virus (MMTV) promoter, Zkscan4 was found to inhibit Gr transactivation by up to 70%, with v-rel reticuloendotheliosis viral oncogene homolog A (Rela) and 12S E1A serving as positive controls (Fig. 5B) given their reported ability to repress Gr transactivation (*25*, *26*). Furthermore, Zkscan4 was still found to repress Gr transactivation with stably transfected MMTV promoters (fig. S6E). However, Zkscan4 did not affect the expression of Gr or the nuclear translocation of Gr (fig. S6, F to H). Htr2a was reported to be a target of Gr (*27*). In the present study, we explored the binding of Gr to the Htr2a promoter in nonstressed *Zkscan4*$^{-/-}$ mice using a ChIP assay. The ChIP-PCR assay demonstrated that the Htr2a promoter region contained two binding sites for Gr in the mouse hippocampus (Fig. 5C, left), and ChIP-qPCR results confirmed that the amount of Gr bound to the promoter of the two Htr2a promoter regions was lower in *Zkscan4*$^{-/-}$ mice than in WT mice (Fig. 5C, right). These results indicated that Zkscan4 inhibits the transcription of Htr2a by directly interacting with the Htr2a promoter and recruiting Gr (fig. S6I).

To further identify which domain of Zkscan4 is responsible for the interaction with Gr, we performed pull-down assays using various glutathione *S*-transferase (GST) fusions of Zkscan4, revealing that full-length Zkscan4 and the N-terminal SCAN domain Zkscan4$_{1-133}$, especially the Zkscan4$_{51-133}$ mutant, could directly bind to Gr (Fig. 5, D and E). Zkscan4$_{1-133}$ attenuated the interaction between full-length Zkscan4 and Gr (Fig. 5, F and G), and Zkscan4$_{1-133}$ repressed the transactivation of Gr (Fig. 5H). Moreover, Zkscan4$_{1-133}$ inhibited luciferase activity under the control of Htr2a (fig. S6J). These results indicated that Zkscan4$_{1-133}$ likely inhibits Htr2a transcription through its direct interaction with Gr.

To explore whether Zkscan4$_{1-133}$ plays a transcriptional regulatory role in Htr2a expression in vivo, we introduced CamkII-driven Zkscan4$_{1-133}$ into the CA3 region of *Zkscan4*$^{-/-}$ mice using an AAV tool (Fig. 5I) and found that it could repress the up-regulation of Htr2a in *Zkscan4*$^{-/-}$ mice at both the mRNA and protein levels, although the level of Htr2a was still slightly greater than that in the WT group (Fig. 5, J to L). Furthermore, Zkscan4$_{1-133}$ improved excitatory

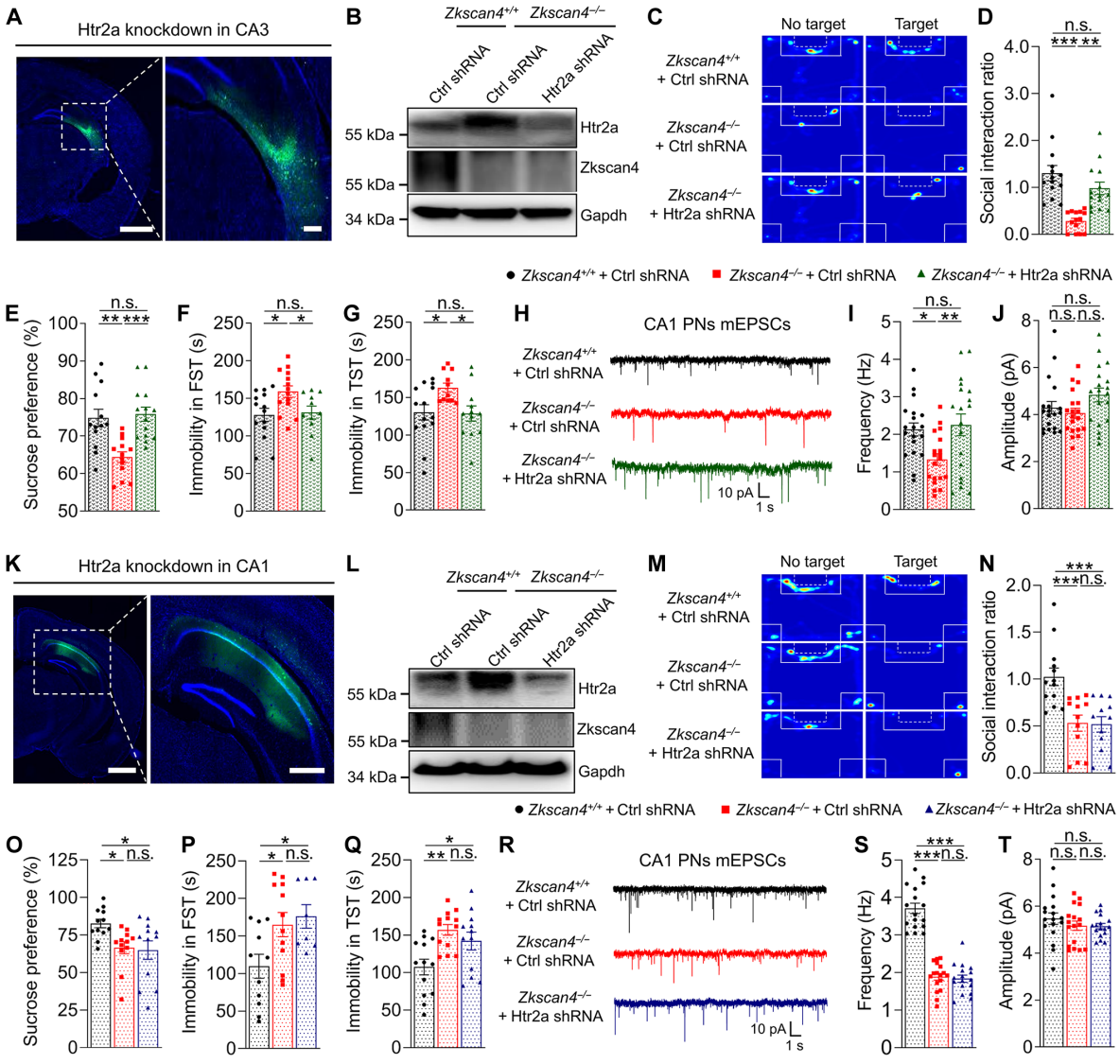

Fig. 4. Genetic knockdown of Htr2a in the CA3 region, but not in the CA1 region, reverses synaptic dysfunction and depression-like behaviors in *Zkscan4*$^{-/-}$ mice. (**A**) Representative image of neurons in the CA3 region of the hippocampus infected with the virus. Scale bars, 1 mm (normal magnification) and 200 μm (high magnification). (**B**) AAV–short hairpin Htr2a (shHtr2a)–EGFP treatment decreased Htr2a expression in *Zkscan4*$^{-/-}$ mice. (**C**) Representative heatmaps showing the amount of time spent in the social interaction test after SCSDS. (**D** to **G**) Htr2a knockdown in the CA3 region reversed SCSDS-induced depression-like behaviors in *Zkscan4*$^{-/-}$ mice, as assessed using a social interaction test, sucrose preference test, forced swimming test, and tail suspension test. (**H**) Representative traces of mEPSCs recorded in hippocampal slices from different groups of mice. (**I** and **J**) Htr2a knockdown in the CA3 region improved the frequency of mEPSCs in CA1 pyramidal neurons in *Zkscan4*$^{-/-}$ mice but did not affect the amplitude of mEPSCs. (**K**) Representative image of neurons in the CA1 region of the hippocampus infected with the virus. Scale bars, 1 mm (normal magnification) and 500 μm (high magnification). (**L**) Htr2a knockdown in the CA1 region decreased Htr2a expression in *Zkscan4*$^{-/-}$ mice. (**M**) Representative heatmaps of time spent in the social interaction test after SCSDS. (**N** to **Q**) Htr2a knockdown in the CA1 region did not affect depression-like behaviors, as assessed using a social interaction test, sucrose preference test, forced swimming test, and tail suspension test. (**R**) Representative traces of mEPSCs recorded in hippocampal slices from different groups of mice. (**S** and **T**) Genetic knockdown of Htr2a in the CA1 region did not affect the frequency and amplitude of mEPSCs in CA1 pyramidal neurons. All the data are presented as the means ± SEMs. One-way ANOVA. **P* < 0.05; ***P* < 0.01; ****P* < 0.001.

synaptic dysfunction (Fig. 5, M to O) and social stress–induced depression-like behaviors in *Zkscan4*$^{-/-}$ mice (Fig. 5, P to T) without affecting locomotion or total fluid intake (fig. S6, K and L). These results indicated that Zkscan4$_{1-133}$ alone could promote stress resistance.

DISCUSSION

The present study showed that hippocampal Zkscan4 was downregulated in both patients with MDD and susceptible mice exposed to CSDS, and we also found that Zkscan4 in the hippocampus was a critical transcription factor in stress coping strategies. Furthermore, Zkscan4 confers resilience to stress-induced depression mainly through its inhibitory effect on the transcription of Htr2a. Dysregulation of CA3, rather than CA1, Htr2a disrupts excitatory synaptic transmission in the hippocampus, ultimately leading to behavioral changes in susceptible individuals, suggesting that CA3 Htr2a might increase the vulnerability to chronic stress–induced depression-like behaviors.

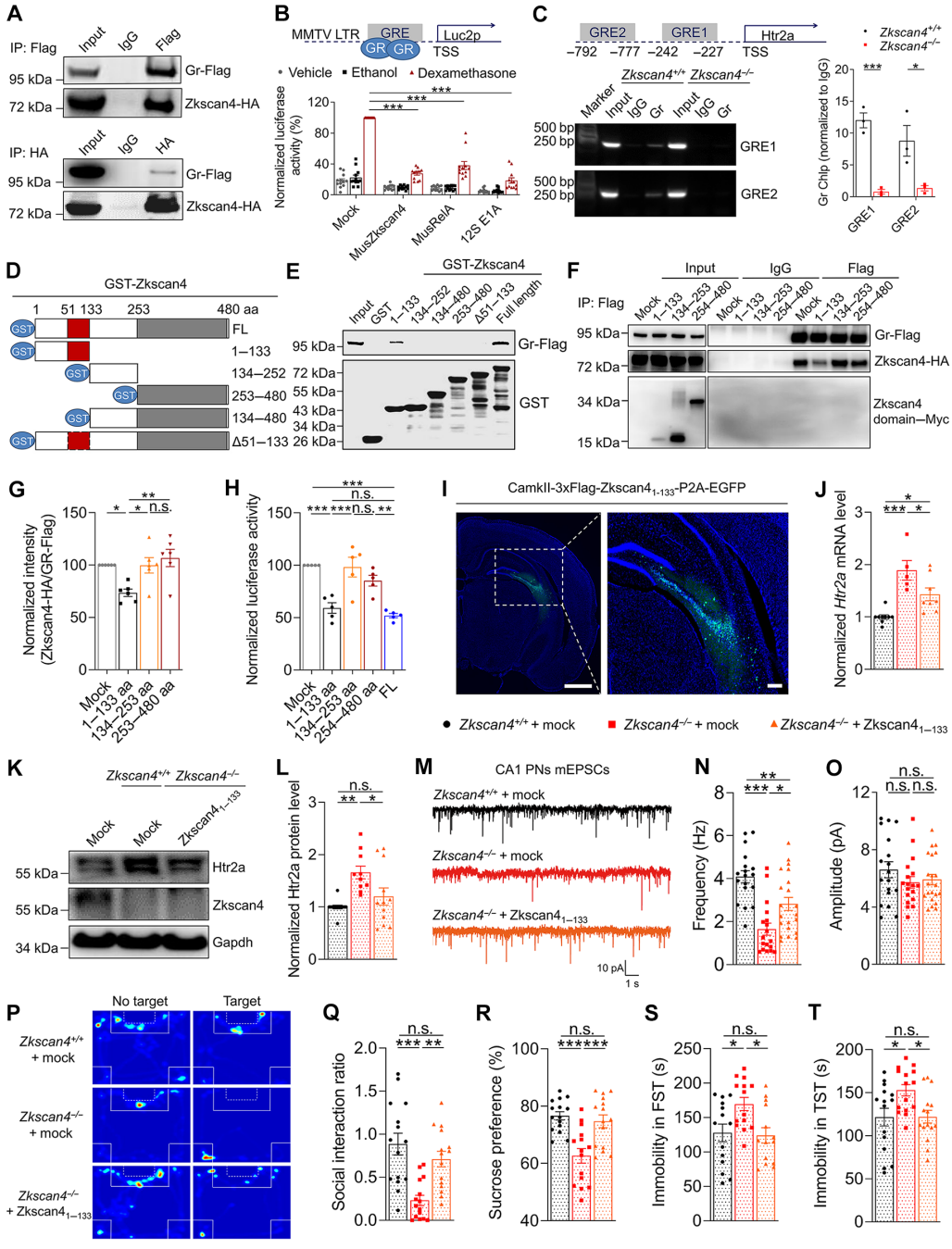

Fig. 5. Zkscan4$_{1–133}$ ameliorated synaptic dysfunction and depression-like behaviors in *Zkscan4*$^{-/-}$ mice through partial inhibition of Htr2a transcription and recruitment of Gr. (**A**) The interaction between Zkscan4 and Gr. HA, hemagglutinin. (**B**) Zkscan4 inhibited the transactivation of Gr signaling. LTR, long terminal repeat. MusZkscan4, mouse Zksca4; MusRela, mouse Rela. (**C**) Decreased Gr binding to the Htr2a promoter in the hippocampus of *Zkscan4*$^{-/-}$ mice in both Gr binding elements (GRE1, −242 to −227; GRE2, −792 to −777). GRE, glucocorticoid response element. (**D**) Schematic representation showing the proteins used for the glutathione *S*-transferase (GST) pull-down assay. GST is the control, and Gr is the target protein. aa, amino acid. (**E**) The N-terminal SCAN domain of Zkscan4 (Zkscan4$_{1–133}$) and full-length (FL) Zkscan4 directly interacted with Gr. (**F** and **G**) Zkscan4$_{1–133}$ inhibited the interaction between Zkscan4 and Gr. (**H**) Zkscan4$_{1–133}$ inhibited Gr transactivation, as assessed using a dual luciferase assay. (**I**) Representative image of neurons infected with control virus in the CA3 region of the hippocampus. Scale bars, 1 mm (normal magnification) and 200 μm (high magnification). (**J**) Htr2a mRNA expression was partly reversed by AAV-CamkII-Zkscan4$_{1–133}$-EGFP injection in *Zkscan4*$^{-/-}$ mice. (**K** and **L**) Western blotting demonstrated that Htr2a up-regulation was partly counteracted by AAV-CamkII-Zkscan4$_{1–133}$-EGFP injection in *Zkscan4*$^{-/-}$ mice. (**M**) Representative traces of mEPSCs recorded in hippocampal slices from different groups of mice. (**N** and **O**) Decreased mEPSC frequency, but not amplitude in the CA1 pyramidal neurons of *Zkscan4*$^{-/-}$ mice, was partly counteracted by AAV-CamkII-Zkscan4$_{1–133}$-EGFP injection in the CA3 region. (**P**) Representative heatmaps showing the amount of time spent in the social interaction test after SCSDS. (**Q** to **T**) AAV-CamkII-Zkscan4$_{1–133}$-EGFP injection in the CA3 region reversed depression-like behaviors, as assessed by the social interaction test, sucrose preference test, forced swimming test, and tail suspension test. All data are presented as the means ± SEMs. Two-way ANOVA and one-way ANOVA. *P < 0.05; **P < 0.01; ***P < 0.001.

The role of transcriptional mechanisms in mediating stress-induced depression has been widely studied in recent years (*28*, *29*). It has been reported that the transcriptional programming driven by zinc finger protein 189 in the prefrontal cortex and orthodenticle homeobox 2 in the ventral tegmental area exerts stress-resilient and antidepressant-like effects (*30*, *31*). In the present study, we found that Zkscan4, a zinc finger transcriptional repressor encoded by a susceptibility gene for MD, was selectively down-regulated in the hippocampi of mice with depression-like behaviors. Our experiments demonstrated that hippocampal Zkscan4 was important for CSDS-induced depression-like behaviors, which may provide further evidence supporting the important role of zinc finger proteins in psychiatric disorders, including MD.

Zkscan4 is a transcriptional repressor belonging to the KRAB-containing zinc finger transcription factor family and is involved in a wide range of biological events, such as genomic imprinting, metabolism, and cell differentiation (*32*). The KRAB domain recruits tripartite motif-containing 28 (Trim28) to form a scaffold for a heterochromatin-inducing complex primarily composed of the histone 3 lysine 9 methyltransferase SET domain bifurcated histone lysine methyltransferase 1, heterochromatin protein 1, and the histone deacetylase–containing nucleosome remodeling deacetylase complex to repress the transactivation of other transcription factors (*33*). ZKSCAN4 suppresses p53, nuclear factor κB, and GR signaling (*24*, *34*, *35*), and we found that mouse Zkscan4 inhibits Gr transactivation. Moreover, forebrain Trim28 knockout mice are vulnerable to stress (*36*), which further supports our finding that *Zkscan4*$^{-/-}$ mice are more susceptible to stress. The present study demonstrated that Htr2a is a common target of both Zkscan4 and Gr and that Gr enrichment in the Htr2a promoter was decreased in *Zkscan4*$^{-/-}$ mice. Our results were similar to those of a prior study showing that corticosterone increases Htr2a expression in the frontal cortex and reduces Gr binding to the Htr2a promoter (*27*). Although our in vivo evidence demonstrated that Zkscan4 is essential for the binding of Gr to the *Htr2a* promoter in nonstressed mice, the exact role of Gr in regulating *Htr2a* expression under chronic stress has not been investigated. Furthermore, whether Gr directly contributes to the suppression of Htr2a expression in the hippocampus and to stress-induced depression-like behaviors remains to be elucidated. In addition, full-length Zkscan4 and its domain Zkscan4$_{1–133}$ play similar roles in the transcriptional repression of Htr2a and stress resistance, suggesting that the peptide Zkscan4$_{1–133}$ might represent an attractive target for depression treatment.

In rat and tree shrew models of chronic restraint stress and chronic social stress, pyramidal neurons in the CA3 region of the hippocampus exhibited significant dendritic atrophy (*37*–*39*), and 5-HT reuptake enhancer tianeptine prevented the dendritic atrophy in CA3 pyramidal neurons caused by repeated restraint stress (*38*). We found that the dendritic morphology of CA3 pyramidal neurons in *Zkscan4*$^{-/-}$ mice was reduced following SCSDS. These findings indicated that *Zkscan4* deletion with the abnormal up-regulation of Htr2a might also increase the susceptibility of CA3 pyramidal neurons to dendritic atrophy. Thus, we speculate that immoderate 5-HT signaling might be involved in the dendritic atrophy in CA3 pyramidal neurons after chronic stress. Moreover, a growing body of evidence has indicated that dysfunction of synaptic transmission, especially excitatory synaptic transmission, may be associated with the pathophysiology of depression (*40*, *41*). Numerous studies have reported that the dendrite length and branching of hippocampal pyramidal neurons, including those in the CA1 and CA3 regions, are reduced (*42*, *43*) and that basal excitatory synaptic transmission at hippocampal CA3-CA1 synapses is decreased after exposure to chronic stress (*44*). Furthermore, the enhanced excitability of hippocampal CA1 pyramidal cells through disinhibition has an antidepressant effect similar to that of ketamine or scopolamine, suggesting the dysfunction of CA3-CA1 synaptic transmission in depression (*45*). In the present study, we found that excitatory synaptic transmission, rather than inhibitory transmission, at hippocampal CA3-CA1 synapses was decreased in *Zkscan4*$^{-/-}$ mice, indicating that these mice are susceptible to stress.

Htr2a has been implicated as a functional candidate in a series of behaviors and neuropsychiatric disorders. Htr2a also plays a role in associative learning or dystonia onset under stressful conditions (*46*, *47*). However, studies on the transcriptional mechanism by which Htr2a is regulated have largely focused on its pharmacological effects (*48*, *49*), and these studies yielded complicated or even paradoxical results (*50*). It has been reported that Htr2a is up-regulated by a variety of stressors (*46*, *51*, *52*), which is consistent with our finding that hippocampal Htr2a was up-regulated in susceptible mice exposed to CSDS compared with that in nonstressed controls and resilient mice. However, the upstream transcriptional regulation of Htr2a by stress is largely unknown. Previous studies have shown that Htr2a in the frontal cortex can be up-regulated via early growth response 3, PHD finger protein 8, and Gr (*27*, *51*, *53*). In the present study, we found that Zkscan4 was an upstream transcriptional repression factor regulating Htr2a expression in response to stress, in which Gr might be a vital corepressor through its interaction with Zkscan4 in the hippocampus. The expression of Htr2a, a common target gene of Zkscan4 and Gr, in the hippocampi of stress-exposed naive *Zkscan4*$^{-/-}$ mice is increased, and the transcriptional repression effect of Zkscan4 is reduced. When *Zkscan4*$^{-/-}$ mice were exposed to subthreshold chronic social stress, Htr2a expression and depression-like behaviors were further increased compared with those of their WT littermates; this result is consistent with reports in the literature indicating that Htr2a is up-regulated in response to stress. Combining the evidence that previous studies have reported, *Htr2a* knockout does not alter the onset or severity of depression-like behaviors induced by chronic stress (*54*, *55*), and we proposed that Htr2a up-regulation, but not *Htr2a* knockout, might be involved in chronic stress–induced depression-like behaviors. Furthermore, we also found reduced Gr enrichment at the Htr2a promoter in *Zkscan4*$^{-/-}$ mice, which is consistent with the finding that maternal immune activation can induce Htr2a dysregulation through Gr (*27*).

Accumulating evidence indicates that classic serotonergic psychedelics (e.g., psilocybin) hold promise as rapid and sustained antidepressants for both patients with MD and animal models primarily through Htr2a activation (*56*–*58*), although this is not supported by all studies (*59*). These findings are inconsistent with our finding that MDL100907, a selective antagonist, improved the synaptic dysfunction and stress susceptibility of *Zkscan4*$^{-/-}$ mice. There are several explanations for this contradiction. First, psychedelics can mediate pharmacological effects through the activation of Htr2a located in cortical and subcortical structures (*60*, *61*), and we found that MDL100907 may have an antidepressant effect mainly through the blockade of Htr2a in the CA3 region in subthreshold stress model. Second, although psychedelics mainly act on Htr2a, they also stimulate other serotonergic receptors, such as Htr1a (*61*). Third, recent studies have indicated that psychedelics exert an antidepressant

effect and enhance synaptic strength, which is not dependent on Htr2a activation, suggesting that Htr2a activation may not be required for an antidepressant response to psychedelics (*62*, *63*). There are also studies supporting our finding that HTR2A down-regulation contributes to the antidepressant-like properties of psychedelics (*17*, *64*, *65*). Recently, a phase 3 randomized double-blind placebo-controlled study showed that lumateperone, a potent HTR2A antagonist and dopamine D2 receptor modulator, improved depression symptoms (*66*). Pharmacological blockade of Htr2a effectively reverses synaptic dysfunction and alleviates subthreshold stress–induced depression-like behaviors in *Zkscan4*$^{-/-}$ mice; however, it fails to rescue chronic stress–induced synaptic dysfunction and depression-like behaviors in WT mice. This discrepancy may stem from differences in stress severity, as the impact of stress on the hippocampus depends on both its duration and intensity (*9*). Another possible explanation is that the treatment duration in WT mice may have been insufficient, as reversing the physiological, behavioral, and molecular effects induced by CSDS requires at least 4 weeks of chronic antidepressant treatment (*67*, *68*). Although Htr2a is essential for the delayed antidepressant response and its transcriptional down-regulation is associated with chronic antidepressant treatment (*69*, *70*), the up-regulation of Htr2a in WT mice with depression-like behaviors may be a consequence, rather than a cause, of CSDS-induced synaptic dysfunction and behavioral abnormalities. Its precise role in the pathogenesis of depression-like behavior in WT mice remains uncertain and requires further investigation.

We demonstrated that Htr2a up-regulation in the CA3 region, but not in the CA1 region, is involved in stress-induced depression-like behaviors in *Zkscan4*$^{-/-}$ mice. This finding aligns with previous reports indicating that the CA3 region is the most vulnerable region for chronic stress (*71*, *72*) and might represent a big step in understanding the role of hippocampal formation in regulating chronic stress–induced depression-like behaviors. However, it remains unclear whether Htr2a functions presynaptically and/or postsynaptically to alter the characteristics of CA3 pyramidal neurons and thereby affects CA3 to CA1 excitatory synaptic transmission, which requires further investigation. Moreover, the involvement of CA3 pyramidal neurons projecting to other targets beyond CA1 pyramidal neurons in depression-like behaviors in *Zkscan4*$^{-/-}$ mice could not be completely excluded. For instance, neural projections from CA3 pyramidal neurons to somatostatin neurons in the dorsolateral septum have been shown to bidirectionally regulate depression-like behaviors (*73*). Another limitation of the present study is whether these changes are specific to pyramidal neurons. Investigating whether inhibitory neurons or glial cells are also affected is an important next step for a more comprehensive understanding of how stress regulates Zkscan4 expression and in which contexts Zkscan4 regulates Htr2a expression. In addition, the CA3-CA1 synaptic transmission was impaired, but spatial learning and memory were normal in *Zkscan4*$^{-/-}$ mice. The possible reason is that the hippocampal SC-CA1 long-term plasticity was not altered in *Zkscan4*$^{-/-}$ mice although the basal synaptic transmission is impaired, which is worthy of further investigation.

In summary, the present study revealed that the transcriptional repressor Zkscan4 was critical for regulating stress-induced depression-like behaviors related to the Zkscan4/Gr-Htr2a axis (fig. S7). *Zkscan4*$^{-/-}$ mice exhibit excitatory transmission dysfunction and stress susceptibility phenotypes (social withdrawal, anhedonia, and despair), and this effect can be rescued by blockade of Htr2a or overexpression of Zkscan4$_{1-133}$ in the CA3 region. Our findings suggest that Zkscan4$_{1-133}$ may represent potential targets for antidepressants.

MATERIALS AND METHODS

Animals

The *Zkscan4*$^{-/-}$ mouse model was established using the CRISPR-Cas9 system by the Nanjing Biomedical Research Institute of Nanjing University (China). Briefly, Cas9 mRNA and single guide RNAs were microinjected into fertilized embryos of C57BL/6J mice. Heterozygous *Zkscan4* mutations in the mice were confirmed using Sanger sequencing. Homozygous *Zkscan4*$^{-/-}$ mice were born from a heterozygous intercross and used for behavioral analyses, with age- and sex-matched WT littermates serving as the control group. All mice were genotyped 2 weeks after birth using PCR with specific primers (forward, 5′-ACTTGCCAGCTGAATTTTCGAG-3′, and reverse, 5′-GGTTCTCTAGCCATTCTGTGC-3′, for *Zkscan4*$^{+/+}$ mice; forward, 5′-ACTTGCCAGCTGAATTTTCGAG-3′, and reverse, 5′-GGTCCTCGTTAGAACTTCTTCAGA-3′, for *Zkscan4*$^{-/-}$ mice), and the animals were housed until weaning. Thy1-GFP were genotyped using PCR with specific primers (forward, 5′-CGGTGGTGCAG-ATGAACTT-3′, and reverse, 5′-ACAGACACACAC CCAGGACA-3′). All mice were housed (five mice per cage) in an environment with a temperature of 23° ± 1°C, a relative humidity of 50 ± 1%, and a light/dark cycle of 12/12 hours (lights were on from 0800 to 2000 every day), with food and water available ad libitum. Seven- to 12-week-old (unless otherwise specified) *Zkscan4*$^{-/-}$ mice and age- and sex-matched WT controls were used for behavioral experiments. All animal studies were approved by the Ethics Committee for Animal Research of Peking University (no. LA2018131) and performed in compliance with Peking University institutional animal care and use committee guidelines and Association for Assessment and Accreditation of Laboratory Animal Care International guidelines.

Behavioral tests

Mouse behaviors were recorded as video files and analyzed with EthoVision XT 8.0 (Noldus, Netherlands) (see the Supplementary Materials for further details).

ZKSCAN4 expression in patients with MD and controls

To compare *ZKSCAN4* mRNA expression between patients with MD and healthy individuals, we obtained microarray data (quantified by Illumina HumanHT-12 v4 BeadChips) from the DLPFC (controls: 97; cases: 111) and hippocampus (controls: 72; cases: 60) of adult controls and patients with MD from dbGaP (accession number phs000979.v3.p2) (*74*). All the participants were of European ancestry. Gene expression intensities were extracted using the Illumina GenomeStudio version 2011.1 software. The data were normalized to $\log_2$ ratios of fluorescent intensities.

In vitro electrophysiological recording

The electrophysiological recording was performed as previously described (*75*). *Zkscan4*$^{-/-}$ mice and their WT littermates (7 to 10 weeks old) were anesthetized with an intraperitoneal injection of 1% sodium pentobarbital (70 mg/kg of body weight) and perfused immediately with an ice-cold cutting solution, which contained 206 mM sucrose, 2.5 mM KCl, 1.25 mM NaH_2PO_4, 26 mM $NaHCO_3$, 10 mM D-glucose, 2 mM $MgSO_4{\cdot}7H_2O$, 2 mM $CaCl_2{\cdot}2H_2O$, 1 mM L-ascorbic acid, and

3 mM sodium pyruvate (oxygenated with 95% O_2 and 5% CO_2, pH 7.2 to 7.4, and 285 to 295 mOsmol). Acute brain slices (350 μm) containing the hippocampus were cut using a vibratome (Leica, VT1200 S) in ice-cold cutting solution. Hippocampal slices were incubated in artificial cerebrospinal fluid (pH 7.2 to 7.4 and 285 to 295 mosmol), which contained 120 mM NaCl, 2.5 mM KCl, 1.25 mM NaH_2PO_4, 26 mM $NaHCO_3$, 10 mM D-glucose, 1.3 mM $MgSO_4{\cdot}7H_2O$, and 2.5 mM $CaCl_2{\cdot}2H_2O$, for 1 hour at room temperature before recording. Whole-cell voltage-clamp recordings of CA1 pyramidal cells were made in a submersion chamber with patch electrodes (3 to 6 megohm resistance) filled with internal solution containing 130 mM $CsMeSO_3$, 2.8 mM NaCl, 5 mM tetraethylammonium chloride, 20 mM Hepes, 0.4 mM EGTA, 2.5 mM MgATP, 0.25 mM Na_3GTP, and 5 mM N-(2,6-Dimethylphenylcarbamoylmethyl)triethylammonium chloride (pH 7.2 and 285 to 295 mosmol). The mEPSC was isolated by adding the γ-aminobutyric acid receptor antagonist picrotoxin (100 μM) and tetrodotoxin (1 μM) to the bath solution, and the mIPSC was isolated by adding the AMPA receptor antagonist 6-cyano-7-nitroquinoxaline-2,3-dione (20 μM), the *N*-methyl-D-aspartate receptor antagonist D-2-amino-5-phosphonovale-rated (50 μM), and tetrodotoxin (1 μM) to the bath solution. All recordings were performed at a holding potential of −60 mV with a MultiClamp 700B amplifier (Molecular Devices, Sunnyvale, CA, USA) under a microscope (infrared differential interference contrast) at room temperature. The data were filtered at 2 kHz, sampled at 10 to 20 kHz, and then acquired using the Clampfit 10 software (Molecular Devices). The data were analyzed using the Mini Analysis Program (Synaptosoft, Decatur, GA, USA) with an amplitude threshold of 0.5 mV (current means picoampere) for mEPSC analysis.

RNAscope in situ hybridization

RNAscope was performed using an RNAscope 2.5 HD Assay (brown or red; ACDBio) according to the manufacturer's instructions. Briefly, coronal brain sections (15 μm) were prepared and hybridized with appropriately designed probes for 1 hour at 40°C with a hydrophobic barrier around the perimeter of each section before further processing.

Viruses

AAV2/9-CamkII-3xFlag-Zkscan4-P2A-EGFP, AAV2/9-CamkII-3×Flag-Zkscan4$_{1-133}$-P2A-EGFP (5×10^{12} viral genomes (v.g.)/ml), and the control virus AAV2/9-CamkII-3×Flag-P2A-EGFP were produced by Shanghai OBiO Technology (China). The short hairpin sequence 5′-GCTCAATTCCAAACTCCTTAA-3′ was used for Htr2a knockdown. The specificity and efficiency of the shRNAs were validated, and high titers of engineered AAVs (AAV2/9-H1-ShHtr2a-P2A; 1.94×10^{13} v.g./ml) were produced by Shanghai OBiO Technology (China). AAV-CamkIIα-hM3Dq(G_q)-EGFP (2×10^{12} v.g./ml) and the control virus rAAV-CamkIIα-EGFP were purchased from BrainVTA (Wuhan, China).

Stereotaxic surgery

The mice were anesthetized with pentobarbital sodium (70 mg/kg, intraperitoneally) and performed as previously described (*75*). A small craniotomy was performed to expose the skull, allowing a small hole to be drilled. AAV (300 nl) was injected into the hippocampus using a 5-μl syringe (Hamilton, USA) at a rate of 50 nl/min. After the injection, the needle was left unremoved for an additional 5 min and then withdrawn slowly. The scalp was sutured, and the mice were placed into their home cages for at least 3 weeks to recover for behavioral analyses. Then, the stereotaxic coordinates for the hippocampus (Anteriorposterior, AP: −1.7, mediolateral, ML: ±1.2, and dorsoventral, DV: −1.5; AP: −2.3, ML: ±1.75, and DV: −1.75; AP: −2.8, ML: ±3.0, and DV: −3.0; and AP: −3.1, ML: ±2.85, and DV: −3.75), the CA1 region (AP: −2.6 mm; ML: ±2.3 mm; and DV: −1.9 mm), and the CA3 region (AP: −2.6 mm; ML: ±2.8 mm; and DV: −3.0 mm) were set. Following electrophysiological experiments, the brains were sectioned and photographed using a confocal microscope (Olympus, FV1200) to validate viral expression or lysate for Western blotting.

RNA sequencing

Total mRNA was extracted from the hippocampus of *Zkscan4*$^{-/-}$ mice and their littermates (controls). High-throughput RNA-seq was performed using Illumina HiSeq 2500 (Illumina, San Diego, CA) at CapitalBio Corporation (Beijing, China), and the raw sequencing data were aligned to the mouse reference genome (GRCm38, mm10). The P value and fold change cutoff value were set at $P < 0.05$ and $|\text{fold change}| > 1.5$, respectively, for the detection of differentially expressed genes using RNA-seq analysis. Pathway analysis ($q < 0.05$) of these up-regulated genes was conducted using The Database for Annotation, Visualization, and Integrated Discovery tools (https://david.ncifcrf.gov/), and the results are provided in the Supplemental Materials.

Statistical analysis

All experiments and data analyses were conducted with blinding of the genotypes of the mice. The number of animals or replicates (n) is indicated in the figure legends. All normally distributed data are presented as the means ± SEMs. Statistical comparisons were performed with the appropriate statistical methods, and quantification graphs were generated using GraphPad Prism 9.0, as indicated in the figure legends. Normally distributed data were tested using one- and two-way analysis of variance (ANOVA), followed by post hoc Bonferroni correction for multiple comparisons and unpaired or paired two-sample Student's t test for two-group comparisons. Non-normally distributed data were analyzed using the Mann-Whitney U test or Kruskal-Wallis test for intergroup comparisons, followed by Dunn's multiple comparisons test. The one-sample χ^2 test was used to identify the mice that had a significantly different chance (from the expected 1:1) of achieving an outcome in the tube test. $P < 0.05$ was considered to indicate statistical significance.

Supplementary Materials

The PDF file includes:

Supplementary Text
Figs. S1 to S7
Legend for data S1

Other Supplementary Material for this manuscript includes the following:

Data S1

REFERENCES AND NOTES

1. G. B. D. M. D. Collaborators, Global, regional, and national burden of 12 mental disorders in 204 countries and territories, 1990-2019: A systematic analysis for the Global Burden of Disease Study 2019. *Lancet Psychiatry* **9**, 137–150 (2022).
2. A. J. Rush, M. H. Trivedi, S. R. Wisniewski, A. A. Nierenberg, J. W. Stewart, D. Warden, G. Niederehe, M. E. Thase, P. W. Lavori, B. D. Lebowitz, P. J. McGrath, J. F. Rosenbaum, H. A. Sackeim, D. J. Kupfer, J. Luther, M. Fava, Acute and longer-term outcomes in depressed outpatients requiring one or several treatment steps: A STAR*D report. *Am. J. Psychiatry* **163**, 1905–1917 (2006).
3. I. M. Berwian, J. G. Wenzel, A. G. E. Collins, E. Seifritz, K. E. Stephan, H. Walter, Q. J. M. Huys, Computational mechanisms of effort and reward decisions in patients with depression

and their association with relapse after antidepressant discontinuation. *JAMA Psychiatry* **77**, 513–522 (2020).
4. P. F. Sullivan, M. C. Neale, K. S. Kendler, Genetic epidemiology of major depression: Review and meta-analysis. *Am. J. Psychiatry* **157**, 1552–1562 (2000).
5. A. M. McIntosh, P. F. Sullivan, C. M. Lewis, Uncovering the genetic architecture of major depression. *Neuron* **102**, 91–103 (2019).
6. K. S. Kendler, L. M. Karkowski, C. A. Prescott, Causal relationship between stressful life events and the onset of major depression. *Am. J. Psychiatry* **156**, 837–841 (1999).
7. J. R. Scarpa, M. Fatma, Y. E. Loh, S. R. Traore, T. Stefan, T. H. Chen, E. J. Nestler, B. Labonte, Shared transcriptional signatures in major depressive disorder and mouse chronic stress models. *Biol. Psychiatry* **88**, 159–168 (2020).
8. E. J. Nestler, Role of the brain's reward circuitry in depression: Transcriptional mechanisms. *Int. Rev. Neurobiol.* **124**, 151–170 (2015).
9. J. D. Gray, T. G. Rubin, R. G. Hunter, B. S. McEwen, Hippocampal gene expression changes underlying stress sensitization and recovery. *Mol. Psychiatry* **19**, 1171–1178 (2014).
10. P. Marin, C. Becamel, A. Dumuis, J. Bockaert, 5-HT receptor-associated protein networks: New targets for drug discovery in psychiatric disorders? *Curr. Drug Targets* **13**, 28–52 (2012).
11. K. F. Tanaka, B. A. Samuels, R. Hen, Serotonin receptor expression along the dorsal–ventral axis of mouse hippocampus. *Philos. Trans. R. Soc. Lond. B Biol. Sci.* **367**, 2395–2401 (2012).
12. T. Xu, S. C. Pandey, Cellular localization of serotonin$_{2A}$ (5HT$_{2A}$) receptors in the rat brain. *Brain Res. Bull.* **51**, 499–505 (2000).
13. M. Kato, A. Serretti, Review and meta-analysis of antidepressant pharmacogenetic findings in major depressive disorder. *Mol. Psychiatry* **15**, 473–500 (2010).
14. G. N. Pandey, Y. Dwivedi, H. S. Rizavi, X. Ren, S. C. Pandey, C. Pesold, R. C. Roberts, R. R. Conley, C. A. Tamminga, Higher expression of serotonin 5-HT$_{2A}$ receptors in the postmortem brains of teenage suicide victims. *Am. J. Psychiatry* **159**, 419–429 (2002).
15. K. C. Vadodaria, Y. Ji, M. Skime, A. Paquola, T. Nelson, D. Hall-Flavin, C. Fredlender, K. J. Heard, Y. Deng, A. T. Le, S. Dave, L. Fung, X. Li, M. C. Marchetto, R. Weinshilboum, F. H. Gage, Serotonin-induced hyperactivity in SSRI-resistant major depressive disorder patient-derived neurons. *Mol. Psychiatry* **24**, 795–807 (2019).
16. A. S. Eison, U. L. Mullins, Regulation of central 5-HT$_{2A}$ receptors: A review of in vivo studies. *Behav. Brain Res.* **73**, 177–181 (1996).
17. M. C. Mithoefer, C. S. Grob, T. D. Brewerton, Novel psychopharmacological therapies for psychiatric disorders: Psilocybin and MDMA. *Lancet Psychiatry* **3**, 481–488 (2016).
18. D. M. Howard, M. J. Adams, T. K. Clarke, J. D. Hafferty, J. Gibson, M. Shirali, J. R. I. Coleman, S. P. Hagenaars, J. Ward, E. M. Wigmore, C. Alloza, X. Shen, M. C. Barbu, E. Y. Xu, H. C. Whalley, R. E. Marioni, D. J. Porteous, G. Davies, I. J. Deary, G. Hemani, K. Berger, H. Teismann, R. Rawal, V. Arolt, B. T. Baune, U. Dannlowski, K. Domschke, C. Tian, D. A. Hinds, 23andMe Research Team, Major Depressive Disorder Working Group of the Psychiatric Genomics Consortium, M. Trzaskowski, E. M. Byrne, S. Ripke, D. J. Smith, P. F. Sullivan, N. R. Wray, G. Breen, C. M. Lewis, A. M. McIntosh, Genome-wide meta-analysis of depression identifies 102 independent variants and highlights the importance of the prefrontal brain regions. *Nat. Neurosci.* **22**, 343–352 (2019).
19. N. R. Wray, S. Ripke, M. Mattheisen, M. Trzaskowski, E. M. Byrne, A. Abdellaoui, M. J. Adams, E. Agerbo, T. M. Air, T. M. F. Andlauer, S. A. Bacanu, M. Baekvad-Hansen, A. F. T. Beekman, T. B. Bigdeli, E. B. Binder, D. R. H. Blackwood, J. Bryois, H. N. Buttenschon, J. Bybjerg-Grauholm, N. Cai, E. Castelao, J. H. Christensen, T. K. Clarke, J. I. R. Coleman, L. Colodro-Conde, B. Couvy-Duchesne, N. Craddock, G. E. Crawford, C. A. Crowley, H. S. Dashti, G. Davies, I. J. Deary, F. Degenhardt, E. M. Derks, N. Direk, C. V. Dolan, E. C. Dunn, T. C. Eley, N. Eriksson, V. Escott-Price, F. H. F. Kiadeh, H. K. Finucane, A. J. Forstner, J. Frank, H. A. Gaspar, M. Gill, P. Giusti-Rodriguez, F. S. Goes, S. D. Gordon, J. Grove, L. S. Hall, E. Hannon, C. S. Hansen, T. F. Hansen, S. Herms, I. B. Hickie, P. Hoffmann, G. Homuth, C. Horn, J. J. Hottenga, D. M. Hougaard, M. Hu, C. L. Hyde, M. Ising, R. Jansen, F. Jin, E. Jorgenson, J. A. Knowles, I. S. Kohane, J. Kraft, W. W. Kretzschmar, J. Krogh, Z. Kutalik, J. M. Lane, Y. Li, Y. Li, P. A. Lind, X. Liu, L. Lu, D. J. MacIntyre, D. F. MacKinnon, R. M. Maier, W. Maier, J. Marchini, H. Mbarek, P. McGrath, P. McGuffin, S. E. Medland, D. Mehta, C. M. Middeldorp, E. Mihailov, Y. Milaneschi, L. Milani, J. Mill, F. M. Mondimore, G. W. Montgomery, S. Mostafavi, N. Mullins, M. Nauck, B. Ng, M. G. Nivard, D. R. Nyholt, P. F. O'Reilly, H. Oskarsson, M. J. Owen, J. N. Painter, C. B. Pedersen, M. G. Pedersen, R. E. Peterson, E. Pettersson, W. J. Peyrot, G. Pistis, D. Posthuma, S. M. Purcell, J. A. Quiroz, P. Qvist, J. P. Rice, B. P. Riley, M. Rivera, S. S. Mirza, R. Saxena, R. Schoevers, E. C. Schulte, L. Shen, J. Shi, S. I. Shyn, E. Sigurdsson, G. B. C. Sinnamon, J. H. Smit, D. J. Smith, H. Stefansson, S. Steinberg, C. A. Stockmeier, F. Streit, J. Strohmaier, K. E. Tansey, H. Teismann, A. Teumer, W. Thompson, P. A. Thomson, T. E. Thorgeirsson, C. Tian, M. Traylor, J. Treutlein, V. Trubetskoy, A. G. Uitterlinden, D. Umbricht, S. Van der Auwera, A. M. van Hemert, A. Viktorin, P. M. Visscher, Y. Wang, B. T. Webb, S. M. Weinsheimer, J. Wellmann, G. Willemsen, S. H. Witt, Y. Wu, H. S. Xi, J. Yang, F. Zhang, eQtlgen, 23andMe, V. Arolt, B. T. Baune, K. Berger, D. I. Boomsma, S. Cichon, U. Dannlowski, E. C. J. de Geus, J. R. DePaulo, E. Domenici, K. Domschke, T. Esko, H. J. Grabe, S. P. Hamilton, C. Hayward, A. C. Heath, D. A. Hinds, K. S. Kendler, S. Kloiber, G. Lewis, Q. S. Li, S. Lucae, P. F. A. Madden, P. K. Magnusson, N. G. Martin, A. M. McIntosh, A. Metspalu, O. Mors, P. B. Mortensen, B. Muller-Myhsok, M. Nordentoft, M. M. Nothen, M. C. O'Donovan, S. A. Paciga, N. L. Pedersen, B. Penninx, R. H. Perlis, D. J. Porteous, J. B. Potash, M. Preisig, M. Rietschel, C. Schaefer, T. G. Schulze, J. W. Smoller, K. Stefansson, H. Tiemeier, R. Uher, H. Volzke, M. M. Weissman, T. Werge, A. R. Winslow, C. M. Lewis, D. F. Levinson, G. Breen, A. D. Borglum, P. F. Sullivan, C. Major, Depressive Disorder Working Group of the Psychiatric Genomics, Genome-wide association analyses identify 44 risk variants and refine the genetic architecture of major depression. *Nat. Genet.* **50**, 668–681 (2018).
20. T. D. Als, M. I. Kurki, J. Grove, G. Voloudakis, K. Therrien, E. Tasanko, T. T. Nielsen, J. Naamanka, K. Veerapen, D. F. Levey, J. Bendl, J. Bybjerg-Grauholm, B. Zeng, D. Demontis, A. Rosengren, G. Athanasiadis, M. Baekved-Hansen, P. Qvist, G. Bragi Walters, T. Thorgeirsson, H. Stefansson, K. L. Musliner, V. M. Rajagopal, L. Farajzadeh, J. Thirstrup, B. J. Vilhjalmsson, J. J. McGrath, M. Mattheisen, S. Meier, E. Agerbo, K. Stefansson, M. Nordentoft, T. Werge, D. M. Hougaard, P. B. Mortensen, M. B. Stein, J. Gelernter, I. Hovatta, P. Roussos, M. J. Daly, O. Mors, A. Palotie, A. D. Borglum, Depression pathophysiology, risk prediction of recurrence and comorbid psychiatric disorders using genome-wide analyses. *Nat. Med.* **29**, 1832–1844 (2023).
21. D. F. Levey, M. B. Stein, F. R. Wendt, G. A. Pathak, H. Zhou, M. Aslan, R. Quaden, K. M. Harrington, Y. Z. Nunez, C. Overstreet, K. Radhakrishnan, G. Sanacora, A. M. McIntosh, J. Shi, S. S. Shringarpure, 23andMe Research Team, Million Veteran Program, J. Concato, R. Polimanti, J. Gelernter, Bi-ancestral depression GWAS in the Million Veteran Program and meta-analysis in >1.2 million individuals highlight new therapeutic directions. *Nat. Neurosci.* **24**, 954–963 (2021).
22. S. A. Golden, H. E. Covington III, O. Berton, S. J. Russo, A standardized protocol for repeated social defeat stress in mice. *Nat. Protoc.* **6**, 1183–1191 (2011).
23. S. Shin, O. Kwon, J. I. Kang, S. Kwon, S. Oh, J. Choi, C. H. Kim, D. G. Kim, mGluR5 in the nucleus accumbens is critical for promoting resilience to chronic stress. *Nat. Neurosci.* **18**, 1017–1024 (2015).
24. K. Ecker, A. Lorenz, F. Wolf, C. Ploner, G. Bock, T. Duncan, S. Geley, A. Helmberg, A RAS recruitment screen identifies ZKSCAN4 as a glucocorticoid receptor-interacting protein. *J. Mol. Endocrinol.* **42**, 105–117 (2009).
25. E. Soeth, D. B. Thurber, C. L. Smith, The viral transactivator E1A regulates the mouse mammary tumor virus promoter in an isoform- and chromatin-specific manner. *J. Biol. Chem.* **277**, 19847–19854 (2002).
26. B. A. Burkhart, P. B. Hebbar, K. W. Trotter, T. K. Archer, Chromatin-dependent E1A activity modulates NF-κB RelA-mediated repression of glucocorticoid receptor-dependent transcription. *J. Biol. Chem.* **280**, 6349–6358 (2005).
27. J. M. Saunders, C. Muguruza, S. Sierra, J. L. Moreno, L. F. Callado, J. J. Meana, P. M. Beardsley, J. Gonzalez-Maeso, Glucocorticoid receptor dysregulation underlies 5-HT$_{2A}$R-dependent synaptic and behavioral deficits in a mouse neurodevelopmental disorder model. *J. Biol. Chem.* **298**, 102481 (2022).
28. K. Apazoglou, S. Farley, V. Gorgievski, R. Belzeaux, J. P. Lopez, J. Grenier, E. C. Ibrahim, M. A. El Khoury, Y. C. Tse, R. Mongredien, A. Barbe, C. E. A. de Macedo, W. Jaworski, A. Bochereau, A. Orrico, E. Isingrini, C. Guinaudie, L. Mikasova, F. Louis, S. Gautron, L. Groc, C. Massaad, F. Yildirim, V. Vialou, S. Dumas, F. Marti, N. Mechawar, E. Morice, T. P. Wong, J. Caboche, G. Turecki, B. Giros, E. T. Tzavara, Antidepressive effects of targeting ELK-1 signal transduction. *Nat. Med.* **24**, 591–597 (2018).
29. B. Labonte, O. Engmann, I. Purushothaman, C. Menard, J. Wang, C. Tan, J. R. Scarpa, G. Moy, Y. E. Loh, M. Cahill, Z. S. Lorsch, P. J. Hamilton, E. S. Calipari, G. E. Hodes, O. Issler, H. Kronman, M. Pfau, A. L. J. Obradovic, Y. Dong, R. L. Neve, S. Russo, A. Kazarskis, C. Tamminga, N. Mechawar, G. Turecki, B. Zhang, L. Shen, E. J. Nestler, Sex-specific transcriptional signatures in human depression. *Nat. Med.* **23**, 1102–1111 (2017).
30. C. J. Pena, H. G. Kronman, D. M. Walker, H. M. Cates, R. C. Bagot, I. Purushothaman, O. Issler, Y. E. Loh, T. Leong, D. D. Kiraly, E. Goodman, R. L. Neve, L. Shen, E. J. Nestler, Early life stress confers lifelong stress susceptibility in mice via ventral tegmental area OTX2. *Science* **356**, 1185–1188 (2017).
31. Z. S. Lorsch, P. J. Hamilton, A. Ramakrishnan, E. M. Parise, M. Salery, W. J. Wright, A. E. Lepack, P. Mews, O. Issler, A. McKenzie, X. Zhou, L. F. Parise, S. T. Pirpinias, I. Ortiz Torres, H. G. Kronman, S. E. Montgomery, Y. E. Loh, B. Labonte, A. Conkey, A. E. Symonds, R. L. Neve, G. Turecki, I. Maze, Y. Dong, B. Zhang, L. Shen, R. C. Bagot, E. J. Nestler, Stress resilience is promoted by a *Zfp189*-driven transcriptional network in prefrontal cortex. *Nat. Neurosci.* **22**, 1413–1423 (2019).
32. S. Quenneville, G. Verde, A. Corsinotti, A. Kapopoulou, J. Jakobsson, S. Offner, I. Baglivo, P. V. Pedone, G. Grimaldi, A. Riccio, D. Trono, In embryonic stem cells, ZFP57/KAP1 recognize a methylated hexanucleotide to affect chromatin and DNA methylation of imprinting control regions. *Mol. Cell* **44**, 361–372 (2011).
33. A. Lupo, E. Cesaro, G. Montano, D. Zurlo, P. Izzo, P. Costanzo, KRAB-zinc finger proteins: A repressor family displaying multiple biological functions. *Curr. Genomics* **14**, 268–278 (2013).
34. J. Li, Y. Wang, X. Fan, X. Mo, Z. Wang, Y. Li, Z. Yin, Y. Deng, N. Luo, C. Zhu, M. Liu, Q. Ma, K. Ocorr, W. Yuan, X. Wu, *ZNF307*, a novel zinc finger gene suppresses p53 and p21 pathway. *Biochem. Biophys. Res. Commun.* **363**, 895–900 (2007).

35. C. J. Yu, C. Liang, Y. X. Li, Q. Q. Hu, W. W. Zheng, N. Niu, X. Yang, Z. R. Wang, X. D. Yu, B. L. Zhang, B. L. Song, Z. R. Zhang, ZNF307 (zinc finger protein 307) acts as a negative regulator of pressure overload-induced cardiac hypertrophy. *Hypertension* **69**, 615–624 (2017).
36. J. Jakobsson, M. I. Cordero, R. Bisaz, A. C. Groner, V. Busskamp, J. C. Bensadoun, F. Cammas, R. Losson, I. M. Mansuy, C. Sandi, D. Trono, KAP1-mediated epigenetic repression in the forebrain modulates behavioral vulnerability to stress. *Neuron* **60**, 818–831 (2008).
37. C. R. McKittrick, A. M. Magarinos, D. C. Blanchard, R. J. Blanchard, B. S. McEwen, R. R. Sakai, Chronic social stress reduces dendritic arbors in CA3 of hippocampus and decreases binding to serotonin transporter sites. *Synapse* **36**, 85–94 (2000).
38. A. M. Magarinos, A. Deslandes, B. S. McEwen, Effects of antidepressants and benzodiazepine treatments on the dendritic structure of CA3 pyramidal neurons after chronic stress. *Eur. J. Pharmacol.* **371**, 113–122 (1999).
39. A. M. Magarinos, B. S. McEwen, G. Flugge, E. Fuchs, Chronic psychosocial stress causes apical dendritic atrophy of hippocampal CA3 pyramidal neurons in subordinate tree shrews. *J. Neurosci.* **16**, 3534–3540 (1996).
40. S. M. Thompson, A. J. Kallarackal, M. D. Kvarta, A. M. Van Dyke, T. A. LeGates, X. Cai, An excitatory synapse hypothesis of depression. *Trends Neurosci.* **38**, 279–294 (2015).
41. R. S. Duman, G. K. Aghajanian, Synaptic dysfunction in depression: Potential therapeutic targets. *Science* **338**, 68–72 (2012).
42. B. S. McEwen, C. Nasca, J. D. Gray, Stress effects on neuronal structure: Hippocampus, amygdala, and prefrontal cortex. *Neuropsychopharmacology* **41**, 3–23 (2016).
43. A. Vyas, R. Mitra, B. S. Shankaranarayana Rao, S. Chattarji, Chronic stress induces contrasting patterns of dendritic remodeling in hippocampal and amygdaloid neurons. *J. Neurosci.* **22**, 6810–6818 (2002).
44. H. Qiao, S. C. An, W. Ren, X. M. Ma, Progressive alterations of hippocampal CA3-CA1 synapses in an animal model of depression. *Behav. Brain Res.* **275**, 191–200 (2014).
45. A. J. Widman, L. L. McMahon, Disinhibition of CA1 pyramidal cells by low-dose ketamine and other antagonists with rapid antidepressant efficacy. *Proc. Natl. Acad. Sci. U.S.A.* **115**, E3007–E3016 (2018).
46. K. S. Murnane, Serotonin 2A receptors are a stress response system: Implications for post-traumatic stress disorder. *Behav. Pharmacol.* **30**, 151–162 (2019).
47. J. E. Kim, S. Chae, S. Kim, Y. J. Jung, M. G. Kang, W. Heo, D. Kim, Cerebellar 5HT-2A receptor mediates stress-induced onset of dystonia. *Sci. Adv.* **7**, (2021).
48. D. L. Willins, S. A. Berry, L. Alsayegh, J. R. Backstrom, E. Sanders-Bush, L. Friedman, B. L. Roth, Clozapine and other 5-hydroxytryptamine-2A receptor antagonists alter the subcellular distribution of 5-hydroxytryptamine-2A receptors in vitro and in vivo. *Neuroscience* **91**, 599–606 (1999).
49. S. Bhattacharyya, S. Puri, R. Miledi, M. M. Panicker, Internalization and recycling of 5-HT_{2A} receptors activated by serotonin and protein kinase C-mediated mechanisms. *Proc. Natl. Acad. Sci. U.S.A.* **99**, 14470–14475 (2002).
50. J. Akiyoshi, C. Hough, D. M. Chuang, Paradoxical increase of 5-hydroxytryptamine2 receptors and 5-hydroxytryptamine2 receptor mRNA in cerebellar granule cells after persistent 5-hydroxytryptamine2 receptor stimulation. *Mol. Pharmacol.* **43**, 349–355 (1993).
51. X. Zhao, A. B. Ozols, K. T. Meyers, J. Campbell, A. McBride, K. K. Marballi, A. M. Maple, C. Raskin, A. Mishra, S. M. Noss, K. L. Beck, R. Khoshaba, A. Bhaskara, M. N. Godbole, J. R. Lish, P. Kang, C. Hu, M. Palner, A. Overgaard, G. M. Knudsen, A. L. Gallitano, Acute sleep deprivation upregulates serotonin 2A receptors in the frontal cortex of mice via the immediate early gene *Egr3*. *Mol. Psychiatry* **27**, 1599–1610 (2022).
52. A. M. Maple, X. Zhao, D. I. Elizalde, A. K. McBride, A. L. Gallitano, *Htr2a* expression responds rapidly to environmental stimuli in an *Egr3*-dependent manner. *ACS Chem. Nerosci.* **6**, 1137–1142 (2015).
53. R. M. Walsh, E. Y. Shen, R. C. Bagot, A. Anselmo, Y. Jiang, B. Javidfar, G. J. Wojtkiewicz, J. Cloutier, J. W. Chen, R. Sadreyev, E. J. Nestler, S. Akbarian, K. Hochedlinger, *Phf8* loss confers resistance to depression-like and anxiety-like behaviors in mice. *Nat. Commun.* **8**, 15142 (2017).
54. M. Jaggar, N. Weisstaub, J. A. Gingrich, V. A. Vaidya, 5-HT_{2A} receptor deficiency alters the metabolic and transcriptional, but not the behavioral, consequences of chronic unpredictable stress. *Neurobiol. Stress* **7**, 89–102 (2017).
55. N. V. Weisstaub, M. Zhou, A. Lira, E. Lambe, J. Gonzalez-Maeso, J. P. Hornung, E. Sibille, M. Underwood, S. Itohara, W. T. Dauer, M. S. Ansorge, E. Morelli, J. J. Mann, M. Toth, G. Aghajanian, S. C. Sealfon, R. Hen, J. A. Gingrich, Cortical 5-HT_{2A} receptor signaling modulates anxiety-like behaviors in mice. *Science* **313**, 536–540 (2006).
56. G. M. Goodwin, S. T. Aaronson, O. Alvarez, P. C. Arden, A. Baker, J. C. Bennett, C. Bird, R. E. Blom, C. Brennan, D. Brusch, L. Burke, K. Campbell-Coker, R. Carhart-Harris, J. Cattell, A. Daniel, C. DeBattista, B. W. Dunlop, K. Eisen, D. Feifel, M. Forbes, H. M. Haumann, D. J. Hellerstein, A. I. Hoppe, M. I. Husain, L. A. Jelen, J. Kamphuis, J. Kawasaki, J. R. Kelly, R. E. Key, R. Kishon, S. K. Peck, G. Knight, M. H. B. Koolen, M. Lean, R. W. Licht, J. L. Maples-Keller, J. Mars, L. Marwood, M. C. McElhiney, T. L. Miller, A. Mirow, S. Mistry, T. Mletzko-Crowe, L. N. Modlin, R. E. Nielsen, E. M. Nielson, S. R. Offerhaus, V. O'Keane, T. Palenicek, D. Printz, M. C. Rademaker, A. van Reemst, F. Reinholdt, D. Repantis, J. Rucker, S. Rudow, S. Ruffell, A. J. Rush, R. A. Schoevers, M. Seynaeve, S. Shao, J. C. Soares, M. Somers, S. C. Stansfield, D. Sterling, A. Strockis, J. Tsai, L. Visser, M. Wahba, S. Williams, A. H. Young, P. Ywema, S. Zisook, E. Malievskaia, Single-dose psilocybin for a treatment-resistant episode of major depression. *N. Engl. J. Med.* **387**, 1637–1648 (2022).
57. R. E. Daws, C. Timmermann, B. Giribaldi, J. D. Sexton, M. B. Wall, D. Erritzoe, L. Roseman, D. Nutt, R. Carhart-Harris, Increased global integration in the brain after psilocybin therapy for depression. *Nat. Med.* **28**, 844–851 (2022).
58. L. X. Shao, C. Liao, I. Gregg, P. A. Davoudian, N. K. Savalia, K. Delagarza, A. C. Kwan, Psilocybin induces rapid and persistent growth of dendritic spines in frontal cortex in vivo. *Neuron* **109**, 2535–2544.e4 (2021).
59. R. Carhart-Harris, B. Giribaldi, R. Watts, M. Baker-Jones, A. Murphy-Beiner, R. Murphy, J. Martell, A. Blemings, D. Erritzoe, D. J. Nutt, Trial of psilocybin versus escitalopram for depression. *N. Engl. J. Med.* **384**, 1402–1411 (2021).
60. M. V. Vargas, L. E. Dunlap, C. Dong, S. J. Carter, R. J. Tombari, S. A. Jami, L. P. Cameron, S. D. Patel, J. J. Hennessey, H. N. Saeger, J. D. McCorvy, J. A. Gray, L. Tian, D. E. Olson, Psychedelics promote neuroplasticity through the activation of intracellular 5-HT2A receptors. *Science* **379**, 700–706 (2023).
61. F. X. Vollenweider, K. H. Preller, Psychedelic drugs: Neurobiology and potential for treatment of psychiatric disorders. *Nat. Rev. Neurosci.* **21**, 611–624 (2020).
62. R. Moliner, M. Girych, C. A. Brunello, V. Kovaleva, C. Biojone, G. Enkavi, L. Antenucci, E. F. Kot, S. A. Goncharuk, K. Kaurinkoski, M. Kuutti, S. M. Fred, L. V. Elsila, S. Sakson, C. Cannarozzo, C. Diniz, N. Seiffert, A. Rubiolo, H. Haapaniemi, E. Meshi, E. Nagaeva, T. Ohman, T. Rog, E. Kankuri, M. Vilar, M. Varjosalo, E. R. Korpi, P. Permi, K. S. Mineev, M. Saarma, I. Vattulainen, P. C. Casarotto, E. Castren, Psychedelics promote plasticity by directly binding to BDNF receptor TrkB. *Nat. Neurosci.* **26**, 1032–1041 (2023).
63. N. Hesselgrave, T. A. Troppoli, A. B. Wulff, A. B. Cole, S. M. Thompson, Harnessing psilocybin: Antidepressant-like behavioral and synaptic actions of psilocybin are independent of 5-HT2R activation in mice. *Proc. Natl. Acad. Sci. U.S.A.* **118**, (2021).
64. B. D. Pedzich, M. Medrano, A. Buckinx, I. Smolders, D. De Bundel, Psychedelic-induced serotonin 2A receptor downregulation does not predict swim stress coping in mice. *Int. J. Mol. Sci.* **23**, 15284 (2022).
65. H. Gill, B. Gill, D. Chen-Li, S. El-Halabi, N. B. Rodrigues, D. S. Cha, O. Lipsitz, Y. Lee, J. D. Rosenblat, A. Majeed, R. B. Mansur, F. Nasri, R. Ho, R. S. McIntyre, The emerging role of psilocybin and MDMA in the treatment of mental illness. *Expert Rev. Neurother.* **20**, 1263–1273 (2020).
66. J. R. Calabrese, S. Durgam, A. Satlin, K. E. Vanover, R. E. Davis, R. Chen, S. G. Kozauer, S. Mates, G. S. Sachs, Efficacy and safety of lumateperone for major depressive episodes associated with bipolar I or bipolar II disorder: A phase 3 randomized placebo-controlled trial. *Am. J. Psychiatry* **178**, 1098–1106 (2021).
67. N. M. Tsankova, O. Berton, W. Renthal, A. Kumar, R. L. Neve, E. J. Nestler, Sustained hippocampal chromatin regulation in a mouse model of depression and antidepressant action. *Nat. Neurosci.* **9**, 519–525 (2006).
68. O. Berton, C. A. McClung, R. J. Dileone, V. Krishnan, W. Renthal, S. J. Russo, D. Graham, N. M. Tsankova, C. A. Bolanos, M. Rios, L. M. Monteggia, D. W. Self, E. J. Nestler, Essential role of BDNF in the mesolimbic dopamine pathway in social defeat stress. *Science* **311**, 864–868 (2006).
69. L. Medrihan, Y. Sagi, Z. Inde, O. Krupa, C. Daniels, A. Peyrache, P. Greengard, Initiation of behavioral response to antidepressants by cholecystokinin neurons of the dentate gyrus. *Neuron* **95**, 564–576.e4 (2017).
70. J. H. Meyer, S. Kapur, B. Eisfeld, G. M. Brown, S. Houle, J. DaSilva, A. A. Wilson, S. Rafi-Tari, H. S. Mayberg, S. H. Kennedy, The effect of paroxetine on 5-HT_{2A} receptors in depression: An [^{18}F]setoperone PET imaging study. *Am. J. Psychiatry* **158**, 78–85 (2001).
71. Y. Watanabe, E. Gould, B. S. McEwen, Stress induces atrophy of apical dendrites of hippocampal CA3 pyramidal neurons. *Brain Res.* **588**, 341–345 (1992).
72. Sunanda, B. L. Meti, T. R. Raju, Entorhinal cortex lesioning protects hippocampal CA3 neurons from stress-induced damage. *Brain Res.* **770**, 302–306 (1997).
73. H. Wang, Y. Z. Tan, R. H. Mu, S. S. Tang, X. Liu, S. Y. Xing, Y. Long, D. H. Yuan, H. Hong, Takeda G protein–coupled receptor 5 modulates depression-like behaviors via hippocampal CA3 pyramidal neurons afferent to dorsolateral septum. *Biol. Psychiatry* **89**, 1084–1095 (2021).
74. X. Xiao, C. Zhang, M. Grigoroiu-Serbanescu, L. Wang, L. Li, D. Zhou, T. F. Yuan, C. Wang, H. Chang, Y. Wu, Y. Li, D. D. Wu, Y. G. Yao, M. Li, The cAMP responsive element-binding (CREB)-1 gene increases risk of major psychiatric disorders. *Mol. Psychiatry* **23**, 1957–1967 (2018).
75. Y. Ma, K. Gao, X. Sun, J. Wang, Y. Yang, J. Wu, A. Chai, L. Yao, N. Liu, H. Yu, Y. Su, T. Lu, L. Wang, W. Yue, X. Zhang, L. Xu, D. Zhang, J. Li, *STON2* variations are involved in synaptic dysfunction and schizophrenia-like behaviors by regulating Syt1 trafficking. *Sci. Bull. (Beijing)* **69**, 1458–1471 (2024).

Acknowledgments: We are thankful to K. Zhao from the Third Xiangya Hospital of Central South University for providing plasmid pcDNA3.1-Rela. The data of postmortem samples used for the analyses described in this manuscript were obtained from dbGaP accession number phs000979.v3.p2. **Funding:** This work was supported by the STI2030-Major Projects

(2022ZD0204900), the National Natural Science Foundation of China (82330042, 82471566, 81971283, 82271576, and 82101570), the Changping Laboratory (2021B-01-01), the Regional Innovation and Development Joint Fund of the National Natural Science Foundation of China (U23A20434), the China Postdoctoral Science Foundation (2021M690421), and the Non-profit Central Research Institute Fund of Chinese Academy of Medical Sciences (2023-PT320-08).
Author contributions: K.G.: Writing—original draft, conceptualization, investigation, writing—review and editing, methodology, resources, funding acquisition, data curation, validation, formal analysis, software, project administration, and visualization. Y.Y.: Investigation, writing—review and editing, methodology, resources, validation, and formal analysis. Xiaoxuan Sun: Investigation, data curation, validation, and formal analysis. J.W.: Methodology, resources, data curation, validation, supervision, formal analysis, software, and visualization. Xiaqin Sun: Methodology. T.L.: Investigation, resources, validation, and project administration. L.W.: Conceptualization, writing—review and editing, resources, and funding acquisition. M.L.: Investigation, writing—review and editing, validation, and formal analysis. W.Y.: Conceptualization, writing—review and editing, methodology, resources, funding acquisition, data curation, validation, supervision, formal analysis, software, project administration, and visualization. H.L.: Writing—review and editing, resources, funding acquisition, validation, supervision, and project administration. D.Z.: Writing—original draft, conceptualization, writing—review and editing, methodology, resources, validation, and supervision. J.L.: Writing—original draft, conceptualization, investigation, writing—review and editing, methodology, resources, funding acquisition, data curation, validation, supervision, formal analysis, software, project administration, and visualization. **Competing interests:** The authors declare that they have no competing interests. **Data and materials availability:** The data of postmortem samples used for the analyses described in this manuscript were obtained from dbGaP (www.ncbi.nlm.nih.gov/gap) with accession number phs000979.v3.p2. All other data needed to evaluate the conclusions in the paper are present in the paper and/or the Supplementary Materials.

Submitted 25 June 2024
Accepted 21 April 2025
Published 23 May 2025
10.1126/sciadv.adr2291